A particle cohort study (ParCS) of the impact of glucose and sucrose solutions on the kinetics of starch gelatinization

Lily M.A. Santos O'Keefe[a], Yash Mali[b], John M. Frostad[a,c,*]

[a] *Food Science, University of British Columbia, 2205 East Mall Vancouver, Canada V6T-1Z4*
[b] *Computer Science, University of British Columbia, 2366 Main Mall Vancouver, Canada V6T-1Z4*
[c] *Chemical and Biological Engineering, University of British Columbia, 2360 East Mall Vancouver, Canada V6T-1Z3*

Abstract

Using a Particle Cohort Study (ParCS) apparatus, the swelling kinetics of individual granules for sweet potato, corn, tapioca, and A-type wheat starches were investigated in water, glucose, and sucrose solutions. Building on previous work that introduced an empirical swelling function for four pulse starches, and previous modeling efforts, we extended the analysis to a broader range of starch types and solute environments to explore gelatinization at the single-granule level. For the first time, we found that while the swelling curves can be collapsed onto a master curve with only four model parameters (as shown previously) the shape of the resulting master curves are starch-type dependent and insensitive to these solution conditions. We further showed that swelling rate and intra-sample variability to be intrinsic to starch type and also insensitive to these solution conditions. Also for the first time, we made measurements of the diffusion of water into individual starch granules and found it to be three orders of magnitude lower than what was assumed in previous modeling. Finally, we showed that a previously proposed prediction of the correlation between swelling time and swelling ratio is not born out by our data. Altogether, these insights provide a major advance in our understanding of starch behavior in complex environments, and provide a foundation for improved predictive models in food processing where control over gelatinization is essential.

Keywords: starch gelatinization, swelling kinetics, sugar-starch interactions, ParCS, diffusivity

1. Introduction

Starch is a polysaccharide found in plants, making up a significant portion of the carbohydrate contents [1]. When heated in the presence of excess water, starch undergoes starch gelatinization, an irreversible process. This process is characterized by granule swelling, loss of semi-crystalline internal structure, and an associated increase in viscosity [2]. This is an advantageous process in advanced food processing due to its unique ability to alter food products, governing their stability and texture. As well, the propensity of starches to gelatinize relates to their digestibility and glycemic index, therefore the ability to control gelatinization is similarly significant from a health perspective [3]. Despite the widespread use of starch in various industrial applications, studying this gelatinization behavior remains complex due to the influence of both intrinsic compositional factors and environmental conditions.

Structurally, starch granules are composed of linear amylose and highly branched amylopectin molecules which are made up of chains of glucose units [2]. Starch can generally be classified by their botanical source, in the form of pulse, tuber, root, cereal, and psuedo-cereal starches. These sources differ in several key characteristics, including granule morphology, the amylose-to-amylopectin ratio, granule crystallinity, amylopectin chain length distribution [4, 5], and overall granule composition [6, 7, 8]. These inherent differences affect thermal behavior; for example, starches with higher amylose content are often associated

*Corresponding author: john.frostad@ubc.ca

with higher gelatinization temperatures, while higher protein content is linked to reduced granule swelling capacity [9, 10]. Beyond different starch types, it is common for starch granules of a singular source to exhibit heterogeneity, where a sample can contain a variety of sizes, shapes, and internal structures [11, 12, 13].

Gelatinization is also influenced by its processing conditions, such as the inclusion of other components and ingredients. In particular, adding sugar has been found to cause an increase in the temperature required for gelatinization to occur, the extent of which can differ depending on the molecular weight, structure and concentration of the sugar [14, 15, 16, 17]. The mechanism underlying this effect is not universally agreed upon. Proposed explanations include solute–water interactions that limit water availability for granule swelling, solute–starch interactions that increase intermolecular bonding, and effects related to the sugar glass-transition temperature, below which the solute–water system becomes rigid [17, 18, 19].

In work by Renzetti et al. (2021) [20], consistent increases in gelatinization temperature were observed with increases in concentrations of sugar, while the thermal profiles remained largely unchanged. They suggest here that the inherent molecular mechanism of gelatinization is unaffected by the added solutes, though also observe that sugar ingress into the granule may impact kinetics at higher concentrations. While models have previously explored the specific role of these solute-water interactions [21] in multi-component systems, empirical data on sugar diffusivity on a granule-basis is limited.

To measure the impact of these various factors on gelatinization, several methods are typically employed. Differential scanning calorimetry (DSC) and pasting provide insights into characteristic thermal and rheological transitions. However, as bulk methods, they cannot capture the physical behavior or heterogeneity of individual granules [22, 23]. On the other hand, visualization of starch swelling is typically qualitative and involves discrete samples, rendering it unsuitable to quantify both swelling behavior and thermal behavior within the same set of measurements.

Developments have been made into the temporal resolution of the gelatinization process, utilizing various forms of microscopy with tracking systems to allow for the rapid collection of granule-based data in real-time [24, 25]. Segmenting and tracking starch granule gelatinization using machine learning technology has been employed previously with success, allowing for automatic granule detection across large data sets [26]. The use of single particle imaging has further been applied to the kinetic modeling of starch gelatinization, where the observation of swelling behavior in individual granule measurements enables a quantitative analysis of both swelling kinetics and intra-sample variability. For example, the swelling behaviors of waxy-maize starch granules have been previously studied utilizing similar methods, and described with empirical models [27, 28].

Recently, the intra-sample variability was investigated for four pulse starches [29] with the use of a Particle Cohort Study apparatus (ParCS), a technique involving a flow through chamber coupled with hot stage microscopy [30] that allows for continuous, time-lapse imaging of the entire gelatinization process. Through this method, it was determined that swelling curves from the four types of individual starch granules could each be collapsed onto a universal curve described by a Gompertz function. Additionally, the granules were characterized with two parameters: the swelling rate and swelling time. However, it remains unclear whether the universality of this curve is a result of the similar botanical grouping of the four pulse starches, or if the same observations would be maintained across all starch sources and swelling behaviors.

Building on the results of Mo et al. (2023) [29], Li et al. used experimental data from individual red bean starch granules to refine a mathematical model of gelatinization and use numerical simulation to explore the physical origins of the swelling rate and swelling time [31]. Li et al. were able to generate a mathematical correlation to predict the swelling rate and swelling time directly from the physical properties of the starch. Notably, one key finding of this model was that the swelling rate is entirely determined by the diffusive time scale, and that a diffusion coefficient can be estimated from the measured swelling rate. Further experimental validation is also required to test the robustness of this model, especially across other starch types and systems.

In this study, we employ the ParCS method to monitor gelatinization and quantify the swelling rate and swelling time of individual starch granules from four different botanical sources. Measurements are conducted in water and in two concentrations of both glucose and sucrose. Using this dataset, we seek to address the gaps identified in the literature to first determine if a wider range of starch types (beyond the pulse starches studied previously) also exhibit a universal swelling curve. Second, we seek to determine if

the theoretical predictions from [31] can be validated.

We hypothesize that a universal swelling curve will be observed regardless of starch type, but that the addition of solutes will cause a deviation from the universal curve, consistent with previously observed concentration-dependent changes in swelling kinetics [20]. We further hypothesize that the correlation between physical properties and swelling parameters developed by Li et al. [31] will be validated by the new swelling data, where we expect the diffusive time scale to govern swelling kinetics across starch types. Finally, this work aims to continue progress towards a more complete, data-supported understanding of the fundamentals of gelatinization, and support the use of predictive modeling for optimizing industrial processes and better control of starch behavior in food systems.

2. Materials and Methods

2.1. Materials

Sodium metabisulfite was obtained from MCB (Norwood, Ohio, USA). Hard red spring wheat berries (*Triticum aestivum L.*) and popcorn variety corn kernels (*Zea mays everta*) were sourced from Anita's Organic Mill (Chilliwack, BC, Canada). Garnet variety sweet potatoes (*Ipomoea batatas*) were sourced from A.V. Thomas Produce (Atwater, CA, USA) and cassava root (*Manihot esculenta*) was purchased from Sunlight Farms (Vancouver, BC, Canada).

Food grade glucose (dextrose anhydrous) was obtained from NOW Foods (Bloomingdale, IL, USA) and food grade sucrose was purchased from Red Path (Toronto, ON, Canada). Sucrose solutions were prepared at 0.5 M and 1 M concentrations, while glucose solutions were prepared at 1 M and 2 M, to compare solutions of equivalent monosaccharide units [14, 19]. All solutions were prepared with ultrapure water in 100 mL quantities, allowing the same base solutions to be used for all of the starch types. The ultrapure water used in this study was purified with a PURELAB Chorus 1 water purification system (Elga LabWater, Lane End, England, UK).

Starch Isolation

Three different procedures from the literature were used as a basis for starch isolation, with some modifications to accommodate the different starch types [29, 32, 33]. Sweet potato and cassava tubers were washed, peeled, and cut into approximately 1 inch cubes, while the wheat and corn kernels were kept whole. Each type of raw plant material (200g) was placed in 200 mL of 0.5% sodium metabisulfite solution for 24 hours at 4°C. After soaking, the samples were drained and rinsed 2-3 times with deionized (DI) water in a beaker to rinse off the solution.

Each sample was then combined with 500 mL of fresh DI water and blended using a conventional blender for 5 minutes. In succession, the blended slurry was filtered once with a 500 μm (35 mesh) sieve, and twice using a 149 μm (100 mesh) sieve, retaining the filtrate at each step. After every filtration, the collected residue in the sieve was rinsed with additional DI water until the water ran clear, to aid in extracting any remaining starch. The sieved starch slurry filtrate was left to settle in a beaker at room temperature (approximately 24°C) for 4-5 hours until well-separated into two layers.

The upper liquid of each settled starch suspension was poured off and discarded, and the settled starch precipitate was re-suspended in 40 mL of fresh ultrapure water in 50 mL falcon tubes. The starch was centrifuged at 1500 G for 15 minutes. The resulting supernatant was poured off and the upper, non-white layer was scraped off of the pellet. This centrifugation process was repeated 3 more times. All remaining purified starch was transferred to a 40°C oven and left to dry for 24 hours. The dried starch was ground using a mortar and pestle until very fine.

Starch Granule Characterization

To characterize the starch granules, as well as to validate the diameters measured through image analysis, the particle size distribution of each raw starch type was measured using a MicroTrac Series 5000 Sync Particle Size Analyzer (ATS Scientific Inc, Burlington, ON, Canada). In triplicate, 0.5 $\pm$ 0.005 g of starch was suspended in 20 mL ultrapure water. Each starch type was measured assuming a refractive index

Table 1: Mean diameters for four starches, reported with two methods. Note that the variability reported for laser diffraction is between the mean from different replicates, while that for image analysis is the standard deviation of the full distribution of granules. *a*: reported in [35, 36, 23, 37, 38]

	Corn	**Wheat**	**Sweet Potato**	**Tapioca**
Laser Diffraction (vol. weighted) [μm]	16.54 ± 0.22	16.58 ± 0.32	15.98 ± 0.11	12.88 ± 0.33
Image Analysis (vol. weighted) [μm]	18.19 ± 3.97	21.15 ± 4.36	19.65 ± 5.02	16.72 ± 3.23
Image Analysis (# weighted) [μm]	16.66 ± 2.95	18.04 ± 4.50	15.84 ± 4.37	14.92 ± 2.96
Amylose content[a]	21-28%	23-27%	14-20%	17-21%

(RI) = 1.54, corresponding to the reported RI value for starch granules [34]. The equivalent spherical diameters of the starch granules measured using image analysis (both number- and volume-weighted), the volume-weighted mean diameters obtained from laser diffraction, as well as the amylose content for each of the starch types are reported in Table 1. In addition, the particle size distributions and representative microscopic images are depicted in Figure 1, using diameters from both methods - cumulative distributions are used to compare the two methods in order to eliminate any effects of bin size on the results.

2.2. Particle Cohort Study (ParCS)

A ParCS apparatus was used in this study to monitor the starch granules throughout the entire gelatinization process. In a vial, 0.7 ± 0.2 mg of starch was suspended in either 19 mL of ultrapure water or the respective sugar solution. The water used for samples was recorded to have a pH of 6.1 and no pH adjustments were made to any of the solutions.

To suspend an appropriate amount of starch granules, the vials were briefly shaken, then 3 mL of the suspension was taken up with a syringe and immediately transferred to the ParCS chamber. A view of the chamber and overall experimental set-up are depicted in Figure 2. The suspension was left for several minutes once added to the chamber, in order to allow the starch granules to settle to the lower window.

Each starch sample was heated in the ParCS chamber using the following profile (Equation 1), using a Platinum series universal benchtop PID controller (OMEGA Engineering, Norwalk, CT, USA) to monitor and control the temperature. As soon as the granules were settled and positioned within the chamber, the temperature of the chamber was equilibrated to 50°C for 3 minutes. The temperature was maintained at 50°C for 2 more minutes, and then increased linearly at a rate of about 5.7°C/min. After reaching 90°C, this temperature was maintained for 5 minutes, demonstrated by the following function with T in units of Celcius and t in units of seconds:

$$T = \begin{cases} 50 & 180s \leq t < 300s \\ 0.0952t + 21.43 & 300s \leq t < 720s \\ 90 & t \geq 720s \end{cases} \tag{1}$$

The full gelatinization process was observed for each starch sample, attempting to capture around 100-150 randomly dispersed granules in the field of view. Following manual adjustment and removal of unusable objects, ie. those that were aggregated or layered, approximately 60 starch granules were accurately quantified in each set of images. Notably, the wheat granules only include those considered type A, the larger, lenticular population, with granules >10 μm due to limitations in the microscope resolution that prevent accurate analysis of the smaller type B population. The pixel areas of each granule, extracted by the software were converted to granule diameter (D) using the following formula, assuming a roughly spherical conformation:

$$D = 2\sqrt{\frac{A}{\pi}} \tag{2}$$

Overall, images were captured every 2 seconds, over the full 17 minute (or 1020 s long) heating period, but only every 3rd image was used in subsequent analysis (e.g., one image every 6 seconds).

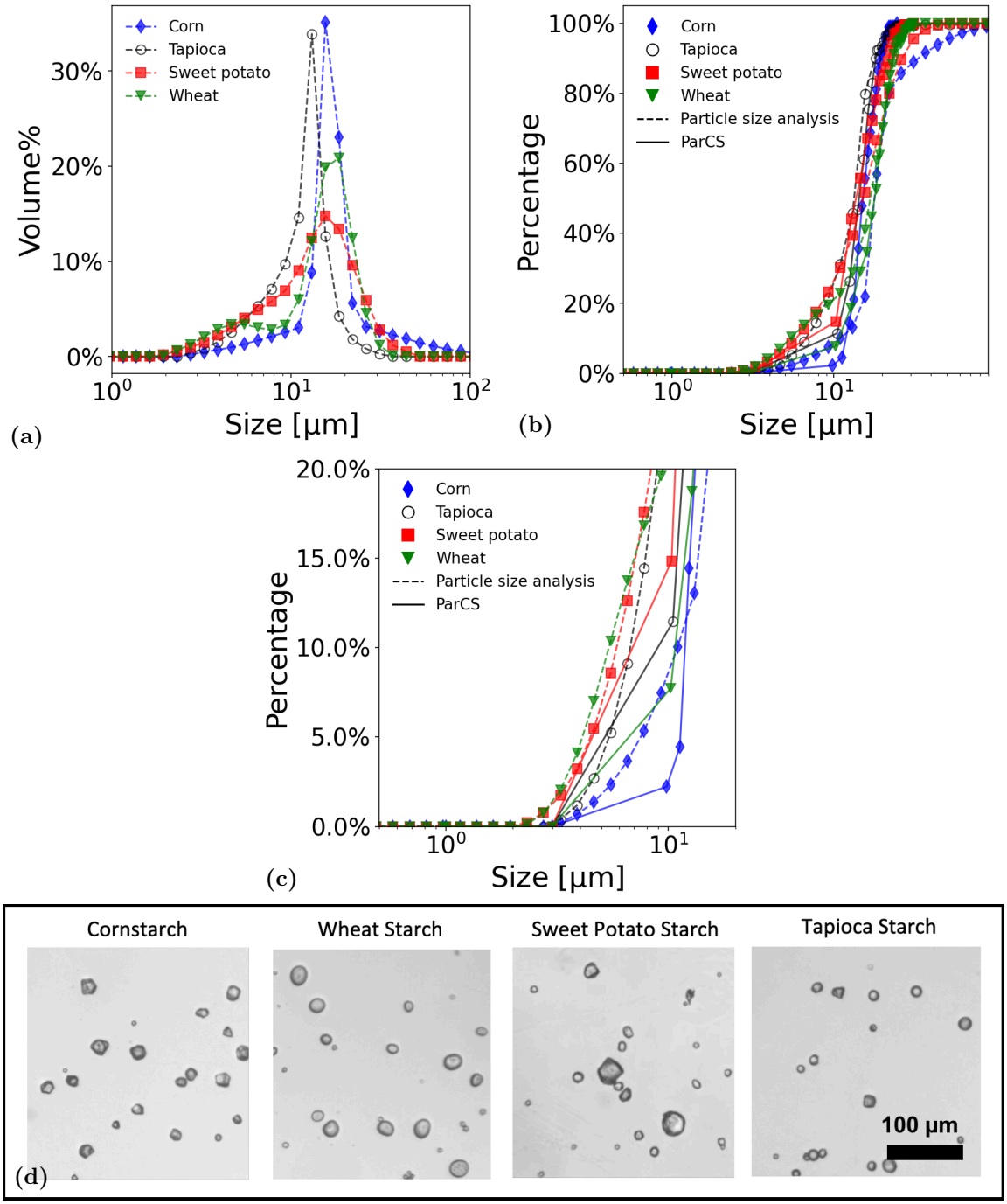

Figure 1: Particle size distributions for particle size analysis represented through volume-weighted size distribution (a) and cumulative distribution of the same data shown in full (b) and zoomed in (c) to better show the differences between measurement method. Representative optical micrographs of each starch type prior to gelatinization (d).

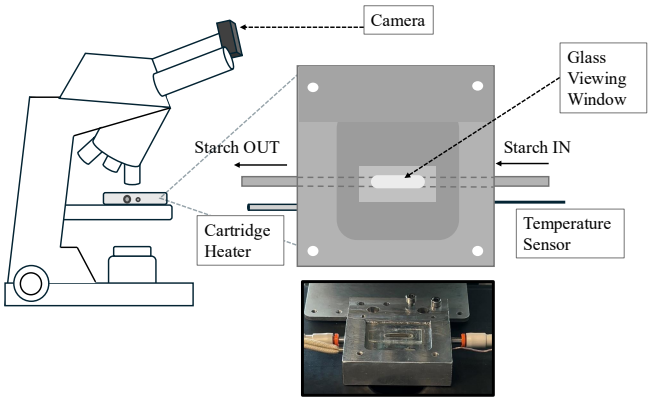

Figure 2: Illustration of the ParCS apparatus and experimental set-up. Readers are directed to [30] for more specific details on the construction of the chamber.

Glass slide treatment

In order to prevent movement caused by convection when the starch granules are heated, a coating is required for the lower glass window. The same procedure as outlined in [29] was followed, where microscopic glass slides were coated with APTES (3-aminopropyltriethoxysilane) to introduce a positive charge and attract the negatively charged phosphate monoester groups present in the starch [39]. Cleaned and dried microscopic slides were first immersed in 1% (v/v) HCl in ethanol solution for 30 minutes then rinsed in ultrapure water. Once dry, the slides were transferred to a solution of 5% (v/v) APTES in acetone for at least 24 hours, rinsed with acetone, then allowed to dry completely.

During this study, the higher molar concentrations of the sugar solutions were observed to result in the appearance of wrinkling of the APTES coating on the glass slide [40, 41]. We hypothesize the osmotic pressure created between the outer high molarity solution and the thin interface between the glass slide and coating layer caused the detachment of a portion of the coating from the slides, and led to a subsequent rippling through the rest of the coating layer. For several tests, this caused a disruption in the gelatinization process and prevented accurate tracking of swelling due to the unpredictable movement of the granules, making the data unusable. For future studies, we suggest using a lower concentration of APTES when preparing a glass slide, to ideally form a thinner initial coating and prevent undesirable film detachment.

2.3. Automated Software

To track the swelling of starch granules over time, custom, deep-learning-based, computer-vision software was used. Based on the successes of transformer-based architectures, we decided to use vision transformer based models to both track and segment each starch particle in the sequence of micrographs. Specifically, we used two stages, both of which are based on the segment-anything-model (SAM) [42].

We first used a fast version of SAM, or "FastSAM" [43] to detect granules in each micrograph. Next, we tracked their bounding boxes using ByteTrack [44], which is integrated within FastSAM. Once we have the bounding boxes, we prompt SAM (which is computationally more intensive) with only the bounding boxes to reduce computation resources. SAM then outputs a binary mask labeling each pixel as either part of the granule or not.

From the binary masks we then find the contours surrounding each granule using the Suzuki-Abe contour finding algorithm [45], followed by the Douglas-Peucker curve simplification algorithm [46] to select a subset of anchor points around each starch granule. After that, we fit the anchor points to a periodic cubic spline

to capture the boundaries and compute the area of each granule. Finally, additional software was developed in-house to enable curation of the data and manual corrections of the anchor points when needed.

2.4. Data Analysis

All data analyses were performed in Python (version 3.11.10). Pairwise Kolmogorov–Smirnov tests were conducted using the SciPy library (version 1.15.2), to assess differences between cumulative distributions of measured values at a significance level of $p = 0.05$.

2.5. Mathematical Models

Past work found favorable results when fitting the starch swelling behavior of four different legumes to a Gompertz function; a sigmoidal growth model [29, 31]. This empirical function is based upon four free parameters, D_f, D_0, k_G, and t_G, where D_f and D_0 can be extracted directly from the intial and final equilibrium diameters in the swelling curves. When non-dimensionalized in terms of diameter and time, the equation is as follows:

$$\frac{D(t) - D_0}{D_f - D_0} = \exp(-e^{-k_G(t-t_G)}). \tag{3}$$

The fitting of data to this equation therefore allows the extraction of parameters: k_G, representing the swelling rate of the individual granules, and t_G, representing the time of at which swelling becomes rapid.

Using these parameters, we can further calculate the swelling temperature of each granule, or T_G. We determine these temperature values by calculating the point at which the diameter exceeds a particular threshold value, previously described by [29]. As done by Mo et al., t_G is defined as the the point at which the dimensionless diameter is equal to 0.05, allowing for a more accurate measurement than what may be achieved if determined qualitatively or "by eye". To find the point at which $\frac{D(t)-D_0}{D_0} = 0.05$, or $D(t) = 1.05D_0$, we substitute this into the original Gompertz function and then rearrange it to solve for the time at which the size has increased by 5%, or $t_{5\%}$,

$$t_{5\%} = t_G - \frac{1}{k_G} \ln \left[- \ln(\frac{0.05 D_0}{D_f - D_0}) \right]. \tag{4}$$

These time values, represented here as $t_{5\%}$, then can used in the equation for the heating profile (Equation 1), to determine the swelling temperature, or T_G.

Testing theory predictions

The results of Li et al. (2025) [31] suggest that k_G, and thus the timescale of gelatinization, can be determined solely by the diffusive time scale. Based on this, we aimed to estimate the diffusion coefficient by fitting the non-dimensionalized data to the Gompertz function. The measured diffusivity is expected to reflect the rate of water transport into the starch granule, which is governed by the resistance of the starch network and its internal morphology. We emphasize that this is only an estimate. The uncertainty arises because the theory has not been quantitatively validated for a system with known material parameters, so the precise dimensionless time corresponding to a particular level of swelling cannot be fixed.

In the present work, the diffusivity is estimated from the swelling rate and the initial diameter, D_0, of the starch granules, both of which can be extracted from fitting the data to the Gompertz function. From the expression used in Li et al. [31], we can write:

$$\kappa = \left(\frac{D_0}{2} \right)^2 k_G. \tag{5}$$

Furthermore, the work by Li et al. found a dependence of t_G on the initial volume fraction of starch within the granule (ϕ_0), the swelling ratio $\left(\frac{D_f}{D_0}\right)$, and the difference between the gelatinization temperature and the initial temperature ($T_G - T_0$).

$$t_G = k_1 \phi_0 \left(\frac{D_f}{D_0} \right)^{k_2} + k_3 (T_G - T_0) \tag{6}$$

From the simulations, the values of various constants were: $k_1 = 15.8$ s, $k_2 = 0.732$, and $k_3 = 2.14$ s/K. In the present work, ϕ_0 cannot be measured for individual granules, so it was assumed to be a constant and equal to 0.586, while 50°C was used for T_0 in every experiment. In this study, we use the experimental data collected to determine the accuracy of this equation in predicting t_G, by comparing the t_G values extracted directly from the data (using Equation 3) to the t_G values calculated from Equation 6.

3. Results and Discussion

3.1. Swelling curves collapse when nondimensionalized

Using the image data analyzed via software, we plotted the swelling curves of individual granules to visualize how their size changes over time during heating and gelatinization. Approximately 200 granules of each starch type were tracked and analyzed. Representative samples for the four starch types, gelatinized in 2M glucose solution as an example, are shown in Figure 3.

Differences are evident in swelling onset time, swelling capacity, and the initial and final granule sizes, both within a single starch type and between different starches. Each starch type also shows apparent differences in the shape of its swelling curves. These differences in shape will be discussed in subsection 3.2.

After obtaining the swelling curves, we fit individual curves to Equation 3 to determine if they also follow a master curve, as observed in Mo et al. [29]. Representative curves for each starch type, gelatinized in water and in the four sugar solutions, were nondimensionalized, time-shifted, and plotted in Figure 4. The mean and standard deviations of the distributions of t_G and k_G are summarized in Table 2. Remarkably, for each starch type, a master curve exists that is agnostic to the five different gelatinization solutions of varying solute and concentration!

These results suggest that the master curve may apply beyond just pulse starches. In light of [29], our findings further indicate that only three material parameters may be sufficient to fully describe swelling for any starch type, regardless of solution. Thus, we partially confirm our hypothesis (see subsection 3.2) that non-pulse starches follow a master swelling curve, but we must reject the idea that solution type alters the shape of the master curve.

Finally, the curves for sweet potato starch gelatinized in water and 1M sucrose (Figure 4B) extend only to a non-dimensionalized time of about 6. This differs from what is observed in the other solutions and starch types, raising several important points. When plotted versus dimensionless time, the extent of the swelling curve (before and after $t = 0$) is influenced by the swelling rate (k_G) and the time shift (t_G), which stretch/compress and shift the zero point of the time axis, respectively. In some cases, truncation occurs simply because the experiment was stopped slightly earlier, highlighting the importance of running the experiment long enough to reach the final swelling diameter. Therefore, non-dimensionalized swelling curves should not be expected to always start and stop at the same time points.

3.2. Swelling-curve shape and swelling ratio are starch-type-dependent

As alluded to in the previous section, there were some noteworthy differences in the *shape* of the collapsed, swelling curves that contradict our hypothesis. For example, corn and sweet potato (Figure 3a/b) appear to fully equilibrate to a final diameter in the latest stages of heating, while the tapioca (Figure 3c) continue swelling gradually until the end of the heating time without an obvious equilibrium. These differences remain noticeable after nondimensionalization and are consistent across all granules and solution types. They reflect variation in equilibrium behavior between starch types. Thus, we must reject our hypothesis that a universal curve can be obtained that has the same shape for all starch types.

A closer look at type-A wheat starch granules in water (Figure 5) reveals an additional subtlety in the swelling curves. When wheat starch was gelatinized in water or in lower sugar concentration solutions (0.5M sucrose and 1M glucose), normal swelling occurred until a dimensionless time of about 4 (see Figure 5a).

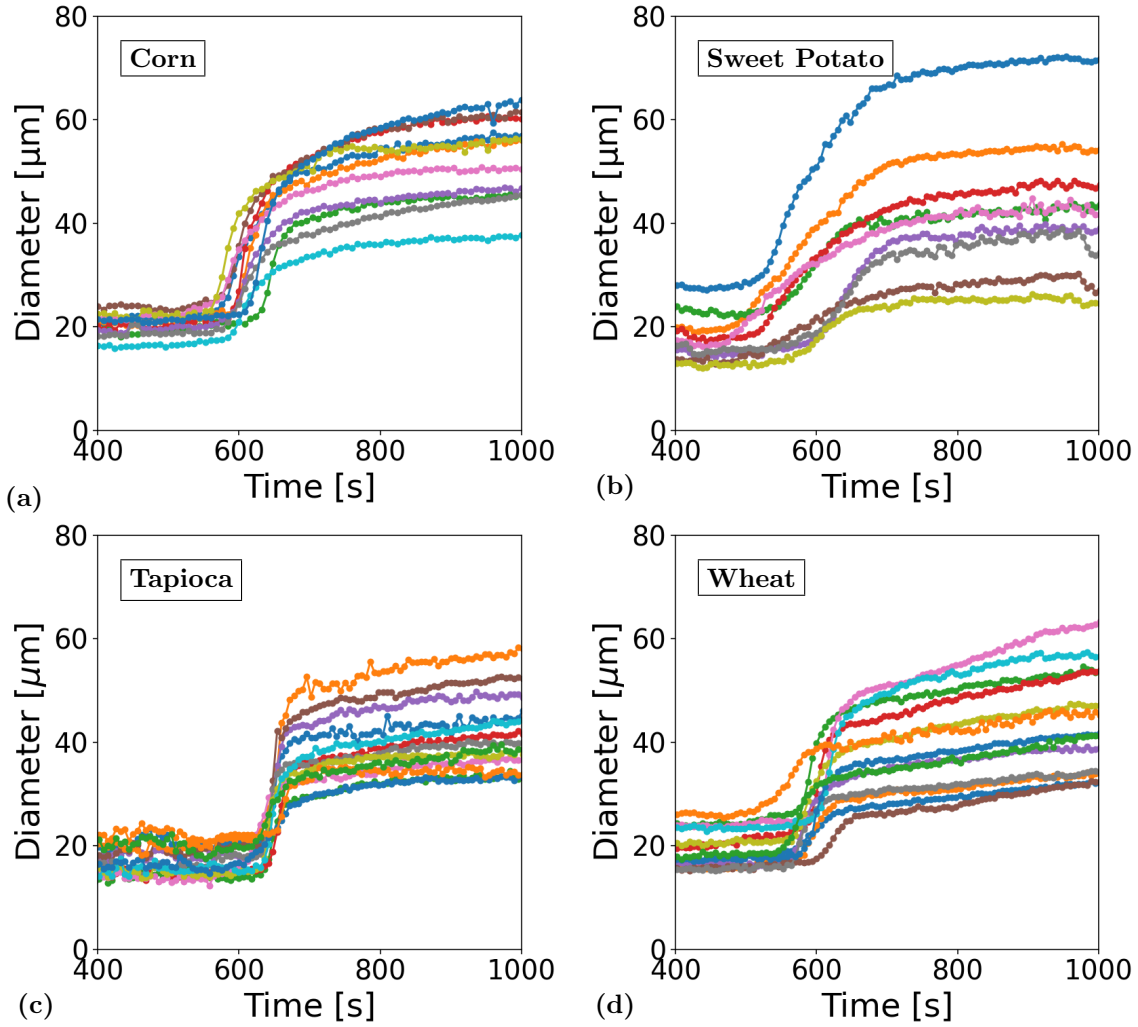

Figure 3: Representative examples of starch-granule, swelling data for (a) corn (b) sweet potato (c) tapioca and (d) wheat, all gelatinized in 2M glucose solution. Each individual line represents a different granule.

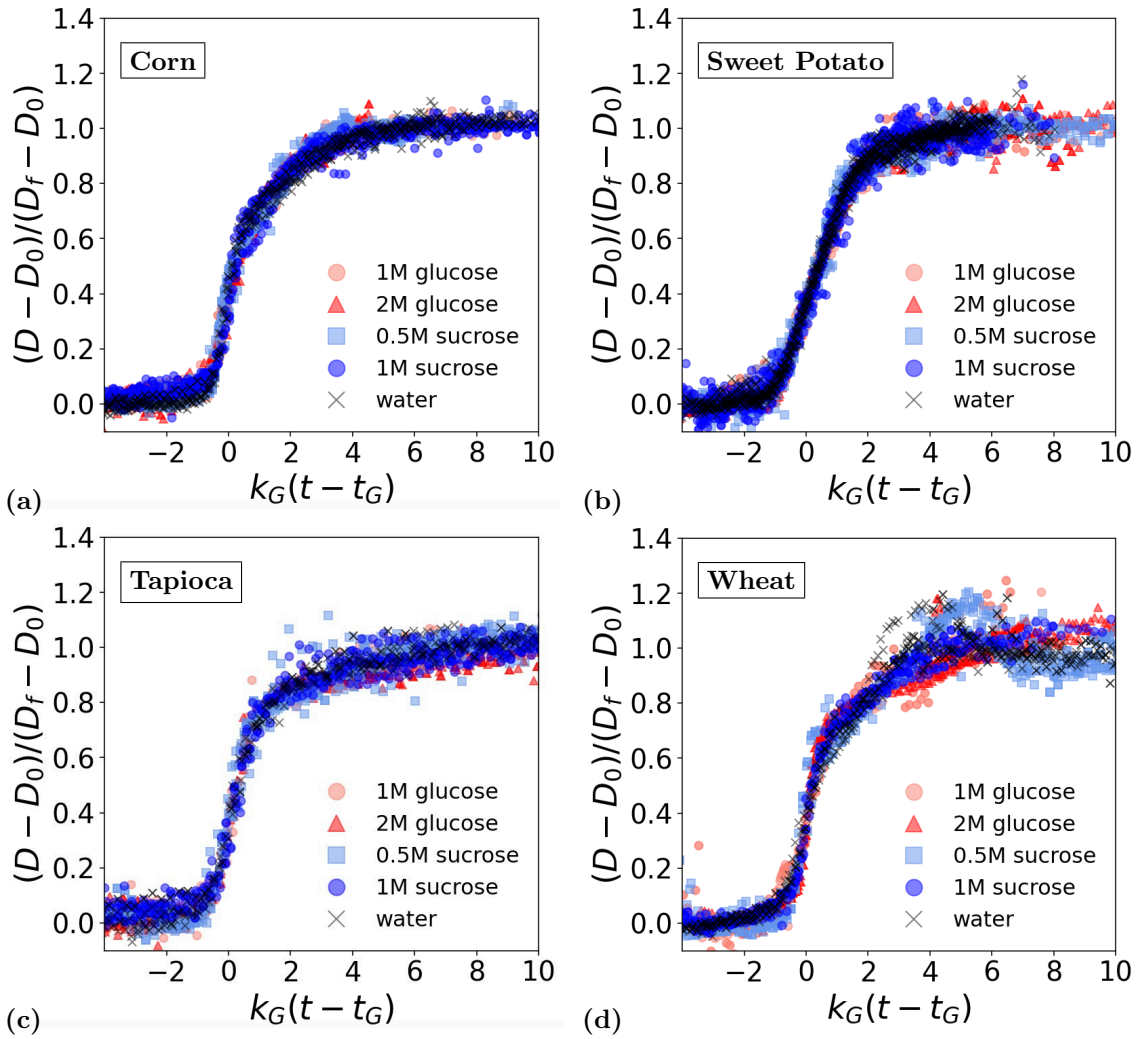

Figure 4: Starch granule swelling data non-dimensionalized and shifted to form a master curve for (a) corn (b) sweet potato (c) tapioca and (d) wheat.

Table 2: Tabulated values of the granule swelling time t_G, swelling rate k_G, swelling ratio D_f/D_0, swelling temperature T_G, and diffusivity κ for each starch gelatinized in five different solutions. The uncertainty intervals reported in this table correspond to the variability between individual granules taken from the standard deviation in the measured distributions, and not the resolution of the measurements which is much more precise.

Starch	**Solution**	t_G [s]	k_G x 10^3 [s^{-1}]	D_f/D_0	T_G [°C]	κ [$\mu m^2/s$]
Corn	Water	527 ± 28	35.9 ± 16	2.14 ± 0.31	68.2 ± 3.3	2.44 ± 1.39
	1 M Glucose	588 ± 25	21.5 ± 7.6	2.77 ± 0.41	70.9 ± 3.2	1.46 ± 0.68
	0.5 M Sucrose	616 ± 23	23.0 ± 11	2.63 ± 0.33	73.8 ± 3.3	1.75 ± 1.20
	2 M Glucose	630 ± 24	26.5 ± 11	2.42 ± 0.28	76.5 ± 3.3	2.00 ± 1.14
	1 M Sucrose	660 ± 25	28.0 ± 9.5	2.26 ± 0.15	80.0 ± 3.3	2.14 ± 0.95
Tapioca	Water	525 ± 20	59.9 ± 33	2.37 ± 0.44	69.1 ± 2.0	3.37 ± 1.91
	1 M Glucose	624 ± 13	46.9 ± 16	2.47 ± 0.63	77.8 ± 1.6	2.23 ± 1.03
	0.5 M Sucrose	587 ± 8	55.0 ± 44	2.37 ± 0.44	74.3 ± 1.5	3.44 ± 2.67
	2 M Glucose	649 ± 15	66.5 ± 35	2.51 ± 0.41	80.8 ± 1.8	3.81 ± 2.73
	1 M Sucrose	650 ± 15	64.2 ± 34	2.35 ± 0.37	80.8 ± 1.9	3.74 ± 2.12
Type-A Wheat	Water	511 ± 37	22.6 ± 15	2.50 ± 0.77	63.0 ± 2.9	1.90 ± 1.71
	1 M Glucose	520 ± 45	23.0 ± 15	2.25 ± 0.50	63.9 ± 3.8	2.16 ± 2.05
	0.5 M Sucrose	536 ± 31	27.3 ± 19	2.22 ± 0.40	66.6 ± 4.0	2.55 ± 2.03
	2 M Glucose	580 ± 29	24.0 ± 14	2.34 ± 0.34	70.7 ± 2.9	1.99 ± 1.14
	1 M Sucrose	612 ± 11	24.0 ± 8.8	2.38 ± 0.23	74.4 ± 2.0	2.53 ± 1.76
Sweet Potato	Water	501 ± 63	17.2 ± 9.7	2.33 ± 0.40	61.0 ± 7.7	0.88 ± 0.61
	1 M Glucose	562 ± 57	21.0 ± 20	2.58 ± 0.37	66.9 ± 7.8	1.42 ± 1.04
	0.5 M Sucrose	565 ± 54	18.5 ± 9.0	2.39 ± 0.48	67.3 ± 8.1	1.15 ± 0.74
	2 M Glucose	633 ± 77	22.9 ± 9.1	2.19 ± 0.34	75.6 ± 8.1	1.50 ± 0.84
	1 M Sucrose	639 ± 66	17.6 ± 9.3	2.14 ± 0.39	75.2 ± 8.3	1.25 ± 0.59

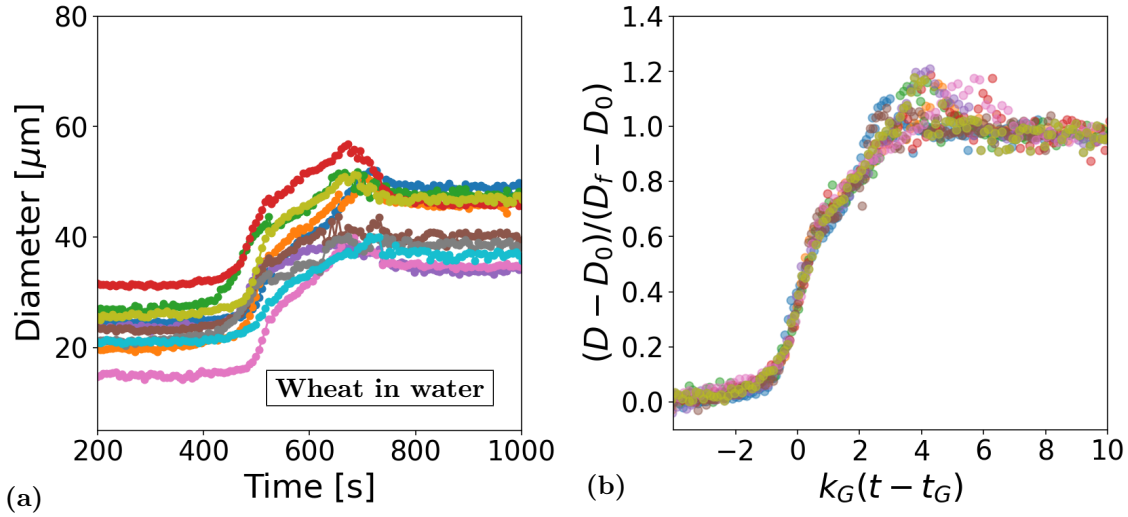

Figure 5: (a) Representative examples of swelling data for wheat gelatinized in water. Each individual line represents a different granule. (b) Data from (a), non-dimensionalized and shifted to a master curve.

After this point, the wheat starch granules began exhibiting an apparent "buckling" behavior where they began folding in on themselves rather than continuing to swell radially.

This buckling behavior has been observed previously and was attributed to an asymmetric distribution of amylose and amylopectin within the granule [47]. Specifically, it was proposed that a higher ratio of amylopectin at the equatorial groove leads to folding of the granules and the formation of a pronounced "saddle" shape [47]. We observed this physical change in wheat starch at temperatures above 70°C. At this point, a certain degree of gelatinization occurs and the granules transform into their amorphous state [48, 49]. Separately, a study observed the collapsing and folding of type-A wheat granules above 85°C, and linked this to the expulsion of amylose molecules from the swollen granules [50].

The non-radial and rapidly changing shape of the granules recorded at the later time points was slightly more difficult to track using the current methods (Figure 5a). Nevertheless, the swelling curves still collapsed after using the Gompertz function as an approximation to determine k_G and t_G, though with somewhat more erratic results at the higher time values (Figure Figure 5b). This is likely because the success of using the Gompertz function to obtain k_G and t_G mainly depends on the region of rapid change.

The "buckling" was not observed when the wheat starch was gelatinized in higher concentrations of sugar, as shown by the granules heated in 2M glucose solution (Figure 3). This suppression of buckling has been observed in previous work, where sugars are shown to decrease the swelling power and amylose leaching of wheat starch granules, implied to be a consequence of the stabilization of the granule structure [51, 52, 53]. Sucrose was also described as having a role in delaying rupture and decreasing amylose leaching, as demonstrated through subsequent microscopic imaging of samples heated to progressively higher temperatures [54].

To our knowledge, we are the first to directly observe through continuous observation of individual granules, that addition of sugar can suppress granule buckling in wheat starch. One possible explanation for the suppression of buckling may be due a shifting of the "buckling temperature" to a higher value, similar to how the gelatinzation temperature is elevated [14]. In that case, buckling was not observed under these experimental conditions. However, it might have occurred if the starch granules had been heated for longer or to a higher temperature. This would align well with a previous study by Bean and Yamazaki (1978) [50], in which they heated their wheat starch up to temperatures of 105°C. They briefly noted the role of sucrose in delaying swelling temperatures and granule collapse, but did not provide data once granule folding was visually identified.

Alternatively, the suppressed buckling may also be connected to the ability of sugar solutions to reduce the swelling ratio. For example, [21] found that a maximum swelling ratio was achieved at 5 wt% and 10 wt% sucrose for rice and maize starches, while concentrations above these values began decreasing the swelling ratio. To check if this is happening here, we can compare the swelling ratios for each starch type and solution. We plotted cumulative distributions of the swelling ratio in Figure 6, and the means and standard deviations of each distribution are also reported in Table 2.

For corn and sweet potato, one notable observation when comparing across solutions is a local maximum in the swelling ratio as the sugar concentration increases. Similar concentration-dependent swelling trends have been reported in Desam et al., and several other studies [55, 20]. At lower concentrations, sugar molecules are said to disrupt the hydrogen-bonded structure of the water molecules, increasing the availability of free water to hydrate the starch granules and act as a better solvent [21]. At higher concentrations, swelling is thought to be inhibited. Water molecules bind increasingly to the sugar, reducing water activity and limiting starch chain mobility within the granule [16, 56].

A final insight is better illustrated in Figure 7, where the starch types are plotted against each other for the same solution. Plotted in this way we clearly see a decrease in variability of the swelling ratio in 2M glucose when compared to the variability in water, for all four starch types. For wheat granules, nearly none exhibited a swelling ratio above 3 in 2M glucose (Figure 7b). By contrast, about 20% of granules exceeded this value in water. Thus, the role of sugar in decreasing the intra-sample variability of swelling ratios for granules of a given starch type is observed for this first time in this work. However, as this was not the intended focus of the current manuscript, we will pursue this finding further in future work.

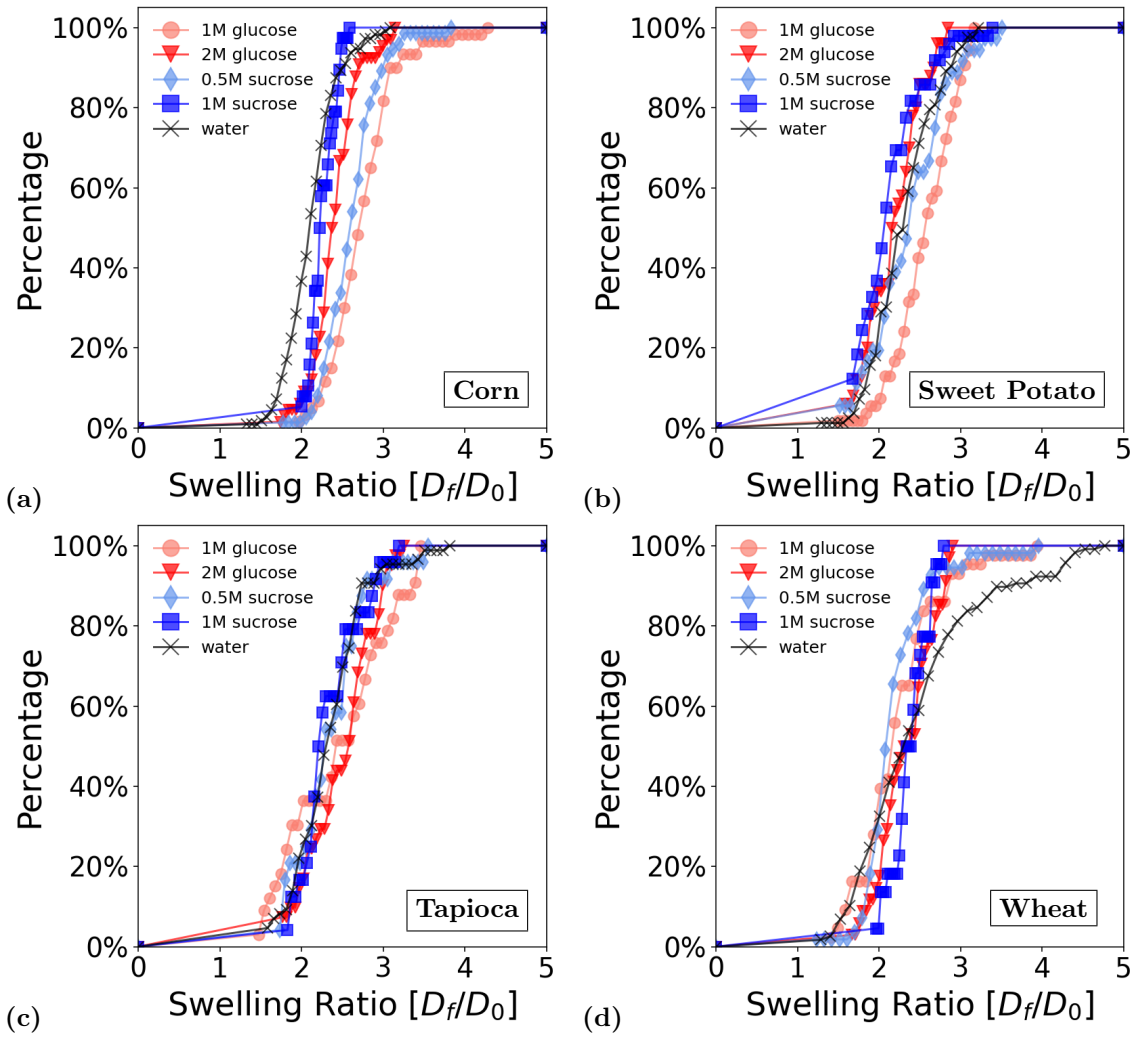

Figure 6: Cumulative distributions of the swelling ratio, D_f/D_0, for (a) corn (b) sweet potato (c) tapioca and (d) wheat, gelatinized in different solutions. Statistical significance: Corn - all pairs were significantly different ($p < 0.05$), except 1M glucose/0.5M sucrose ($p = 0.099$). Sweet potato - all pairs were *not* significantly different ($p > 0.05$) except 1M glucose/2M glucose, 1M glucose/1M sucrose, and 1M glucose/water ($p < 0.05$). Tapioca - all pairs were *not* significantly different, except 1M glucose/water ($p = 0.029$). Wheat - 1M glucose/1M sucrose, 1M glucose/water, 1M glucose/0.5M sucrose, and 0.5M sucrose/water were significantly different ($p < 0.05$).

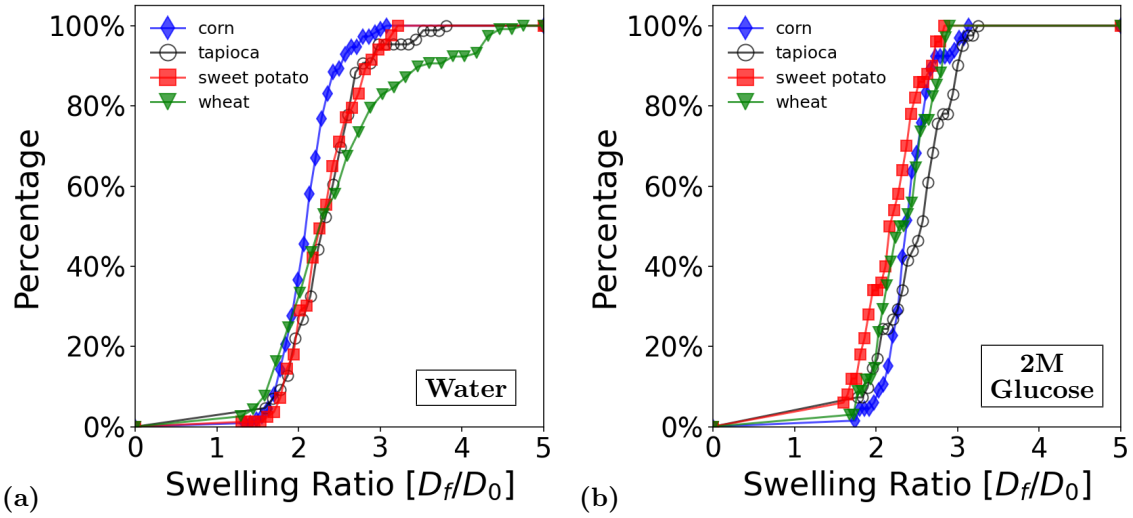

Figure 7: Cumulative distributions of the swelling ratio, D_f/D_0, for starches gelatinized in (a) water and (b) 2M glucose solutions. Note, the data are the same as in Figure 6. Statistical significance: Water - all pairs are significantly different ($p < 0.05$), except sweet potato/tapioca and sweet potato/wheat ($p > 0.05$). 2M glucose - all pairs are significantly different ($p < 0.05$), except wheat/corn, wheat/tapioca, and wheat/sweet potato ($p > 0.05$).

3.3. Sugar causes starch-dependent and solute-dependent increases in swelling temperature

Having demonstrated that the presence of glucose and sucrose as solutes does not alter the shape of the swelling curves, we next analyzed their influence on the swelling temperature. The swelling temperature of the granules, or T_G, was calculated using Equation 4 and Equation 1, and then the cumulative distribution of T_G for each starch type in each solution was plotted in Figure 8. The means and standard deviations of each distribution are also reported in Table 2.

For all four starch types, adding either sugar increased the swelling temperature. The effect became stronger as the solute concentration increased. This was the expected result and is consistent with measurements of DSC endotherms that show a shift to a higher temperature with added sugar [14, 57, 19, 58, 59]. Thus we can proceed to analyze the data further for insights that may help with developing models of gelatinization.

While the overall, qualitative impact of sugar on gelatinization temperature was as expected, there were some noteworthy quantitative differences between different starches. For corn and wheat, sugar type affected T_G. Sucrose appeared to have a stronger effect than the equivalent glucose solution (Figure 8a/d). Both of these starches generally exhibit a very low variability in their T_G values, which is evident from the steepness of the cumulative distributions. The tapioca starch granules also exhibit low variability in their T_G, but the relative effect of solute type is not consistent with corn and wheat (Figure 8c).

On the other hand, sweet potato differs yet again from the other starches, as it exhibited a much greater variability in T_G (Figure 8b). The increased temperature variability was consistent across all solution conditions. This suggests it may be an intrinsic property of the starch source, as also noted by [27]. In addition, while the concentration of the solutes had an impact on the increase of T_G, it was striking to observe no difference between the two sugar types at the same saccharide equivalence.

Some studies have found that solute molecular size strongly affects the onset gelatinization temperature, possibly due to more available hydroxyl groups [19, 58]. Other studies report negligible differences when comparing solutions at equivalent saccharide unit concentrations [57]. Different starch types interact with sweeteners differently, depending on their structure.

Starches with higher ratios of short amylopectin chains, such as wheat and corn, are unable to crystallize fully, allowing more bonds to form with sugar molecules [57]. Consequently, it is possible that unique interactions occurring between the different starch types and the sweeteners were being observed. A more

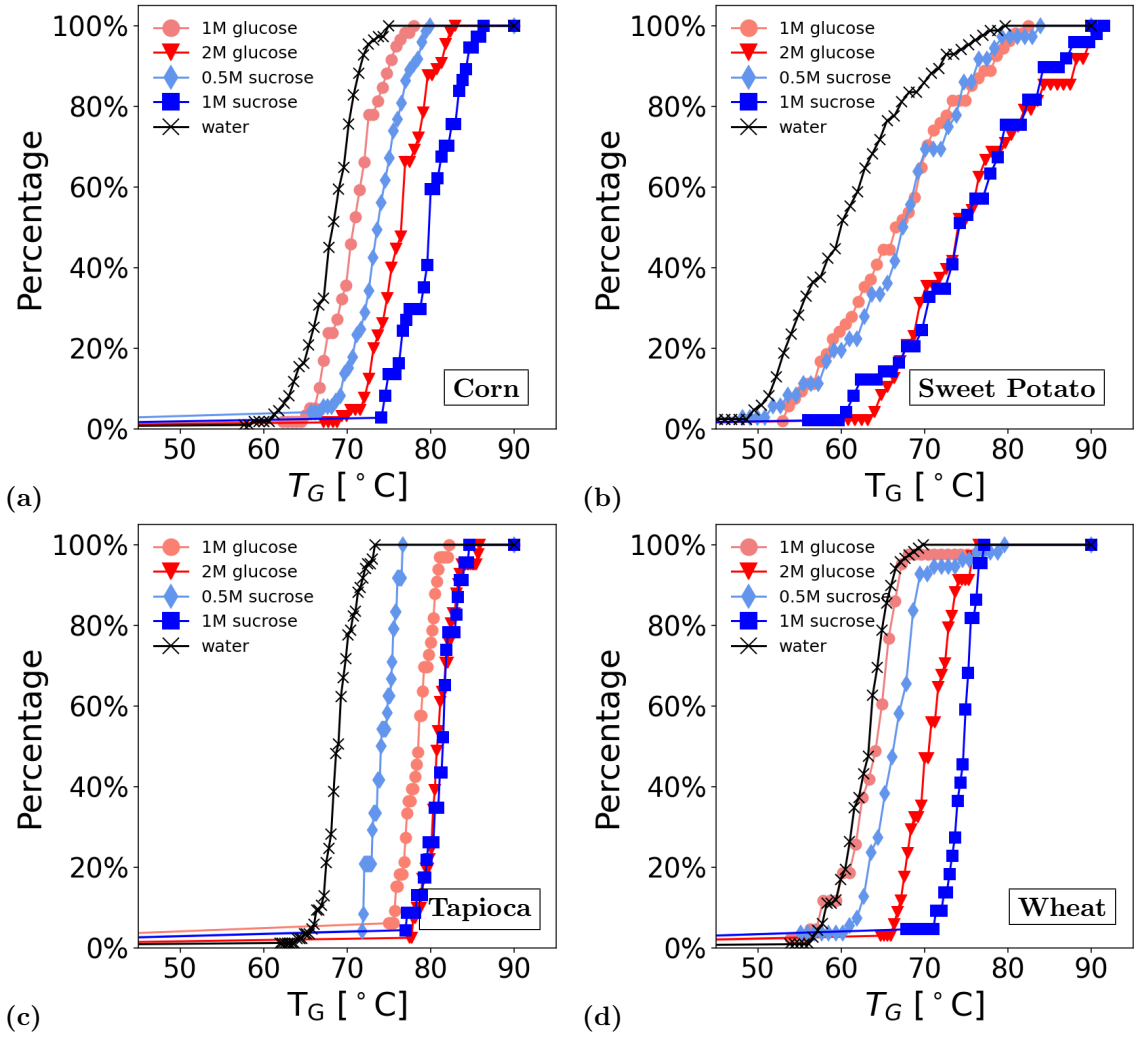

Figure 8: Cumulative distributions of the swelling temperature T_G for (a) corn (b) sweet potato (c) tapioca and (d) wheat, gelatinized in different solutions. Statistical significance: Corn - all pairs are significantly different ($p < 0.05$). Sweet potato - all pairs are significantly different ($p < 0.05$), except 1M glucose/0.5M sucrose and 2M glucose/1M sucrose ($p > 0.05$). Tapioca - all pairs are significantly different ($p < 0.001$), except 2M glucose/1M sucrose ($p = 0.74$). Wheat - all pairs are significantly different ($p < 0.05$), except 1M glucose/water ($p = 0.29$).

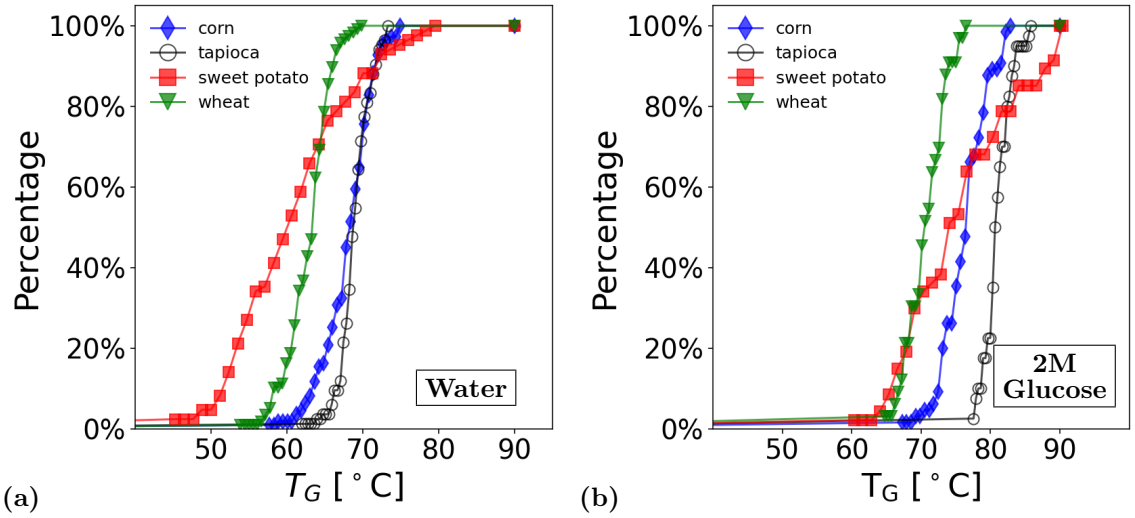

Figure 9: Cumulative distributions for the swelling temperature T_G of starches gelatinized in (a) water and (b) 2M glucose solutions. Note, the data are the same as in Figure 8.

consistent effect might have been observed if lower molecular weight solutes were compared with larger ones, such as oligosaccharides or some artificial sweeteners [60, 57, 59]. This comparison remains for future work.

Figure 9 displays the same data as Figure 8, but directly compares the different starches gelatinized in the same solution using water and 2M glucose as examples. Plotted in this way, we can more clearly see the differences in T_G, and in the variability of the starch granules. Notably, both corn and tapioca have the highest T_G values, wheat starch has the lowest, and the sweet potato starch granules have a much greater variability in T_G compared to the other types as previously noted.

Tapioca exhibits relatively higher T_G values, likely due to its amylopectin architecture. Its more ordered crystalline structure requires more thermal energy to disrupt the amylopectin regions [61]. Across all solutions, the relationship among the four starches is generally consistent. The shape of the cumulative distribution is similar for all starch types but shifted to higher temperatures when comparing gelatinization in 2M glucose to water.

In the context of traditional DSC measurements, the variability within a sample can be inferred from calculating the range, defined as the difference between the onset temperature of gelatinization and the conclusion temperature of the endothermic transition [62]. If taken to be synonymous to the variabilities reported in the current study, we find similarities to gelatinization temperatures observed in literature. Previous work found that the ranges for starch gelatinized in water, sucrose, or sodium chloride were not significantly different for native corn, wheat, and potato starches [63]. This aligns with the minimal changes in variability observed in our study across different solutions.

In separate work, sweet potato starch gelatinization temperatures have shown to be highly dependent on several factors, including the specific variety of sweet potato, its growing conditions, and region of cultivation. Reported ranges in the gelatinization temperature vary widely, from 11°C - 29°C [64, 65]. Samples that have greater ranges in gelatinization temperature are attributed to having a heterogeneous distribution of a-, b-, and c- type crystalline structures across a single starch population, making it logical for the high variability reported in this work to be linked to the starch source itself.

As a final point, we conclude that the quantitative effect of adding a solute when gelatinizing starch produces a result that is both starch dependent and solute dependent. This shows that more work is needed to understand the fundamental impact of solutes. The change in rank order of starch T_G upon adding solutes suggests potential for tuning gelatinization temperature through product formulation. By extension, the best starch type for a particular application may depend on the solutes that will be needed. We posit that a better fundamental understanding will lead to predictive models for this purpose.

3.4. Sugar has minimal impact on swelling rate

In addition to shifting the swelling temperature, the addition of sugar to the gelatinization solution could also impact the rate of swelling, or k_G. If adding sugar delays the onset of swelling to higher temperatures, it might also slow the swelling rate. This slowing is not obvious from the nondimensionalized swelling curves.

A slower swelling rate would appear only as a smaller k_G value. Cumulative distributions for the reciprocal of the swelling rate ($1/k_G$) are plotted for each starch type gelatinized in the 5 different solutions in Figure 10. We chose to use the reciprocal of k_G because it presents the data in the form of a time scale, allowing for a more intuitive interpretation where larger values indicate a slower swelling behavior.

A careful review of Figure 10 reveals that for all four starch types, sugar type and concentration demonstrate only a slight impact on the swelling rate. The variance of the distribution of swelling rates does not change and there is no apparent trend in terms of the influence of sugar type or concentration on the mean swelling rate. Although statistically significant differences were observed between some solution types, the associated effect size remains relatively minimal as depicted by the closely overlapping cumulative distributions. Figure 11 displays the same data as Figure 10, but directly compares the different starches gelatinized in the same solution, with the examples of water and 2M glucose solution.

For starches gelatinized in water (Figure 11b), tapioca had the most rapid swelling rate, followed by corn starch, wheat starch, and then sweet potato starch, whose distribution has the slowest swelling rate overall (Figure 11b). The same rank order is also observed for the 2M glucose solution, though the difference between the corn, sweet potato and wheat starches narrows slightly, primarily due to changes in the swelling rate of corn. Overall, swelling rate appears more dependent on starch type than solution type. This suggests it is tied to an intrinsic property of starch, largely unaffected by solutes. The fact that swelling rate is unaffected despite changes in swelling temperature is counterintuitive. This provides an important clue about the underlying mechanisms.

In contrast to the present work, there have been several observations that might have signaled a stronger effect of sugar on granule swelling rate. For example, as we previously described in subsection 3.2 when discussing swelling ratio, researchers have cited the role of sugar in disrupting the interactions between water molecules and starch granules thus impacting the ability of starch to reach its complete swelling capacity [21, 55, 20]. However, these other studies investigated granule swelling behavior more indirectly through bulk measurements of swelling power, solubility, viscosity, and other rheological parameters.

Therefore, prior work cannot be compared directly to the present work. For example, swelling power measures the extent of water absorption by calculating the ratio of swollen granule mass to dry mass [66], whereas k_G is a kinetic parameter measuring the speed at which this water is absorbed. For those that have quantified the swelling rate of individual granules, they have primarily compared differences in starch swelling behavior due to differences in heating profiles for a single starch type, rather than varying the starch or solute type [27, 28].

We speculate that the rapid swelling rate of tapioca starch is due to one or both of two factors related to its granular microstructure. First, tapioca starch has a relatively low amylose content, where common varieties fall within a generally narrow range of approximately 16-22% [38, 67]. Starches with high amylose content may swell more slowly. This is thought to result from interactions with amylopectin backbones and the formation of helical structures that impede transformation [68]. Second, relative to the other three starch types, tapioca starch contains minimal non-starch components, which include proteins, lipids, and phosphorus [67]. These components may inhibit swelling by forming complexes with amylose, reducing water availability, or acting as cross-linking agents [6, 7, 8].

Because of the likelihood that swelling rate is primarily dependent on the starch composition, we suggest that it is an important parameter for describing the material properties of starch. In addition, it may provide a convenient and practical means of quantitatively differentiating starches from different species and cultivars. Naturally, more work is needed to relate the mean and variance of the distribution of swelling rates to specific performance metrics of interest to applications.

3.5. Diffusivity can be extracted from the swelling rate

In this subsection, for the first time, we present experimental estimates of the diffusivity of water in starch based on swelling of individual starch granules. This is made possible by the recent discovery of Li

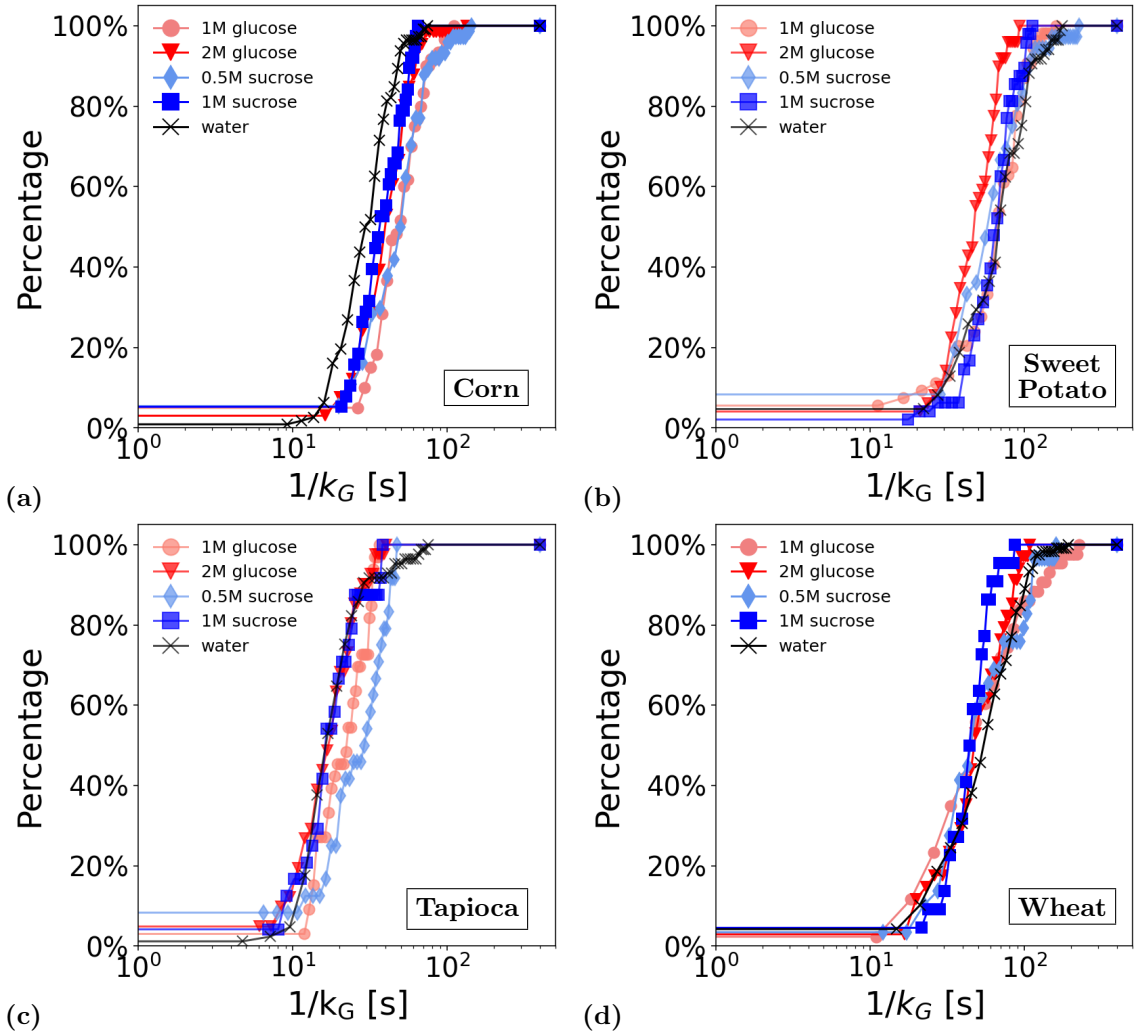

Figure 10: Cumulative distributions of the reciprocal of the swelling rate k_G for (a) corn (b) sweet potato (c) tapioca and (d) wheat, gelatinized in different solutions. Statistical significance: Corn - all pairs were significantly different ($p < 0.05$), except 1M glucose/2M glucose, 1M glucose/0.5M sucrose, and 2M glucose/1M sucrose ($p > 0.05$). Sweet potato - pairs were *not* significantly different ($p > 0.05$), except 2M glucose/water, 2M glucose/1M glucose, 2M glucose/0.5M sucrose, and 2M glucose/1M sucrose ($p < 0.05$). Tapioca - pairs were *not* significantly different, except for 1M glucose/water, 0.5M sucrose/2M glucose, 0.5M sucrose/1M sucrose and 0.5M sucrose/water ($p < 0.05$). Wheat - pairs were *not* significantly different, except for water/0.5M sucrose and water/1M sucrose ($p < 0.05$).

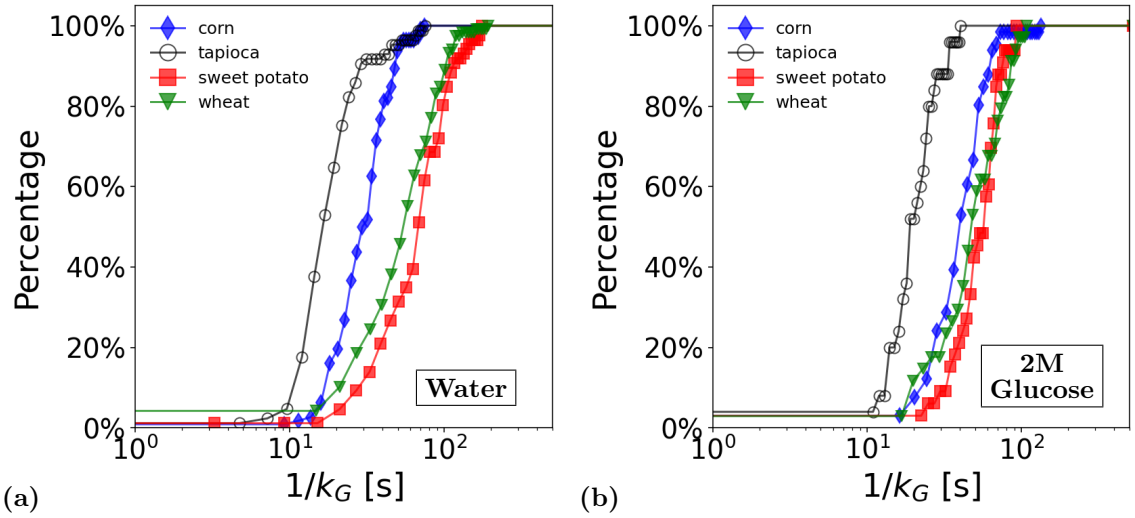

Figure 11: Cumulative distributions for the reciprocal of swelling rate k_G for starches gelatinized in (a) Water and (b) 2M glucose. Note, the data are the same as in Figure 10. Statistical significance: Water - all starch types are significantly different from one another ($p < 0.05$). 2M glucose - all starch types are significantly different from one another ($p < 0.05$).

et al., through numerical simulations, that the swelling rate (k_G) is equal to the diffusion rate as given in Equation 5. Cumulative distributions of diffusivity values are shown for each of the four starch types in Figure 12, and the means and standard deviations of each distribution are also reported in Table 2. Similar to the swelling rate, the diffusivity is relatively unchanged due to solution type and concentration, with no clear trends.

Our estimates of the diffusion rate during swelling contradict the assumption in [31]. That assumption proposed that the self-diffusion coefficient of water determines the diffusion rate. The self-diffusivity of water molecules has been reported as being 2230 μm^2/s at 25°C [69], while the self-diffusion coefficient of monosaccharides and disaccharides in water were reported to range from 153 to 222 μm^2/s at 25°C and 30 wt% [70].

All values measured in this study range from 0.13 to 15 $\mu m^2/s$. This is two to three orders of magnitude lower than reported diffusion coefficients for sugar and water. This is contrary to the notion that water enters starch granules primarily through pores in the starch, where it would be the self-diffusion of water that is most important. Thus, we must consider that diffusion of water directly into the starch matrix is the primary mode of mass transfer during swelling.

Previously, measurements in the literature that reliably measured the diffusivity of water into starch have studied diffusivity in starch films, where water sorption methods are used to look at changes in water content over a drying period [71, 72, 73]. Those studies have reported diffusivities ranging from 100 to 4000 $\mu m^2/s$ across varying experimental conditions, which is a factor of 10-100 times larger than what we measured in intact starch granules. This discrepancy highlights that different transport mechanisms may govern water-in-starch diffusion when comparing bulk and granule-level systems.

These findings suggest much lower mobility within the starch granule matrix. This has important implications for understanding the mechanisms of gelatinization and structural changes during swelling. For example, it has been suggested that the diffusivity of water in starch granules is dependent on the internal cross-link density and polymer ordering of the starch molecules themselves, and is insensitive to the presence of external solutes, at least in the form of the low molecular weight sugars used in these experiments [13]. Additionally, these findings imply that the clear changes observed in gelatinization temperature with increased sugar concentration (Figure 8) were not governed by diffusion effects, perhaps allowing for the distinction of external and internal factors that impact the onset of swelling, with those that impact swelling kinetics.

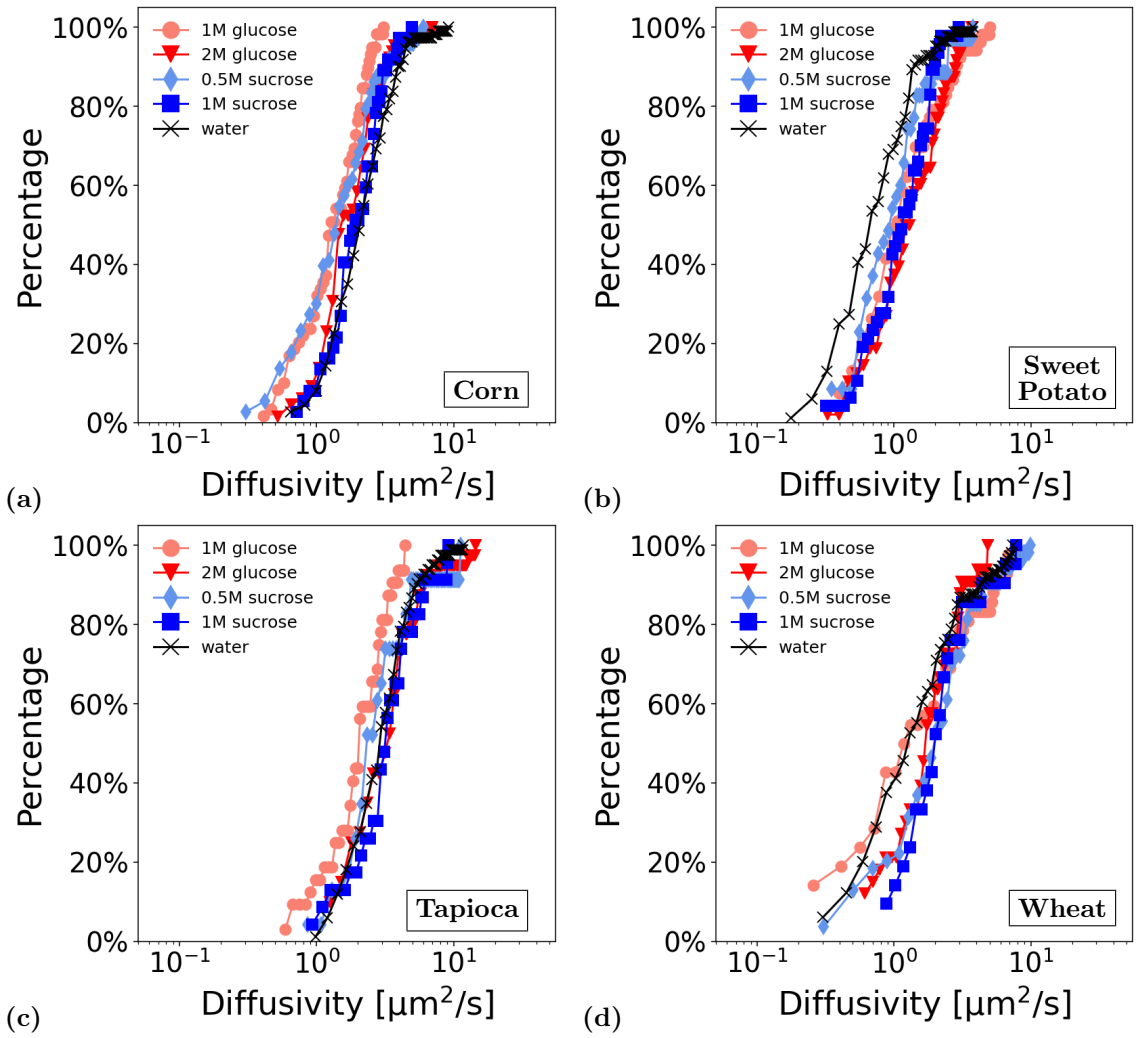

Figure 12: Cumulative distributions of the diffusion coefficient κ for (a) corn, (b) sweet potato, (c) tapioca, and (d) wheat starches gelatinized in different solutions. Statistical significance: Corn - pairs were significantly different ($p < 0.05$), except 1M sucrose/water, 1M sucrose/2M glucose, and 1M glucose/0.5M sucrose ($p > 0.05$). Sweet potato - starch in water was significantly different from all sugar solutions ($p < 0.05$). Tapioca - all pairs were *not* significantly different, except for 1M glucose/2M glucose, 1M glucose/1M sucrose, and 1M glucose/water ($p < 0.05$). Wheat - pairs were *not* significantly different, except 1M glucose/1M sucrose and 0.5M sucrose/water ($p < 0.05$).

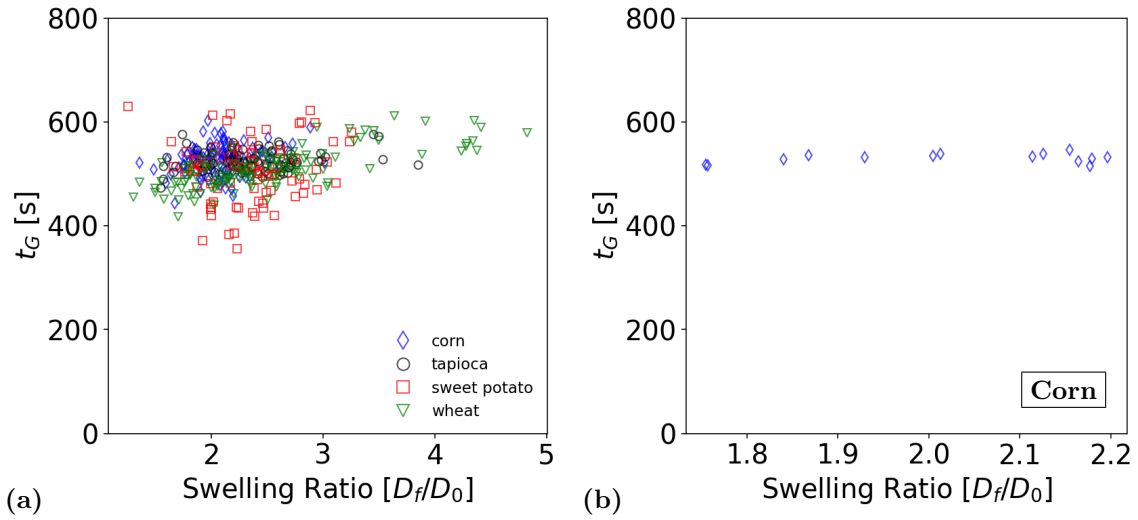

Figure 13: Swelling time t_G vs. swelling ratio D_f/D_0 for (a) the four starches gelatinized in water, and (b) for just corn starch granules with a swelling temperature of $T_G = 68.5 \pm 0.5$°C (b).

3.6. Partial validation of theoretical predictions

Now that we had characterized these four starches with a variety of physical parameters, we sought to use our experimental data to assess the predictive model proposed by Li et al. (2025) [31] in their Equation 39. For the sake of this comparison, only the data collected for the starches gelatinized in water are analyzed, to match the conditions used in Li et al., where the addition of solutes and changes in the gelatinization conditions were not considered. We first plotted the swelling ratio, D_f/D_0, against the swelling time, t_G (Figure 13a) and expected to find a power-law relationship if there is agreement with the numerical simulations. Evidently, there seems to be no clear dependence of swelling ratio on t_G for any of the starches analyzed.

Although there appears to be little correlation between t_G and swelling ratio, we examined this more closely. In development of the theoretical model, each parameter was treated as an independent parameter and varied only while holding all of the other parameters constant. In the real data (Figure 13a), each granule can have its own unique set of parameters. In particular, the different granules have different swelling temperatures.

So, one might instead hypothesize that a correlation between swelling ratio and t_G may be observed if T_G was held "constant". To control for T_G, we selected 15 corn granules from the dataset for which $T_G = 68.5 \pm 0.5$°C, and plotted this subset in Figure 13b. This subset shows even more clearly that there is no relationship between the swelling time and the swelling ratio. Consequently, this partially invalidates the model prediction from ref. [31] and instead suggests that swelling ratio is completely independent of swelling time.

A second prediction of the model that we aim to assess is the relation between $T_G - T_0$ and t_G, where we expected see a linear relationship. Recall that in this work, T_0 is fixed at 50°C, similar to the simulations. As shown in Figure 14, we did, in fact, observe a clear linear relationship for all four starch types. This linear relationship is logical given that T_G and t_G are both determined based on when initial and rapid swelling are observed, respectively.

In terms of correlation coefficients we found there to be the strongest correlation for corn starch ($r = 0.910$), with a slightly weaker relationship observed with the tapioca starch granules ($r = 0.738$) and sweet potato starch granules ($r = 0.797$). Conversely, the wheat starch granules had a lower correlation coefficient of $r = 0.251$. A possible explanation for the much weaker correlation for wheat starch might be that the final diameter, D_f, is less well defined as described earlier in subsection 3.2, making it more difficult to fit the data to the Gompertz function. This would directly influence Equation 4 and the calculation of T_G.

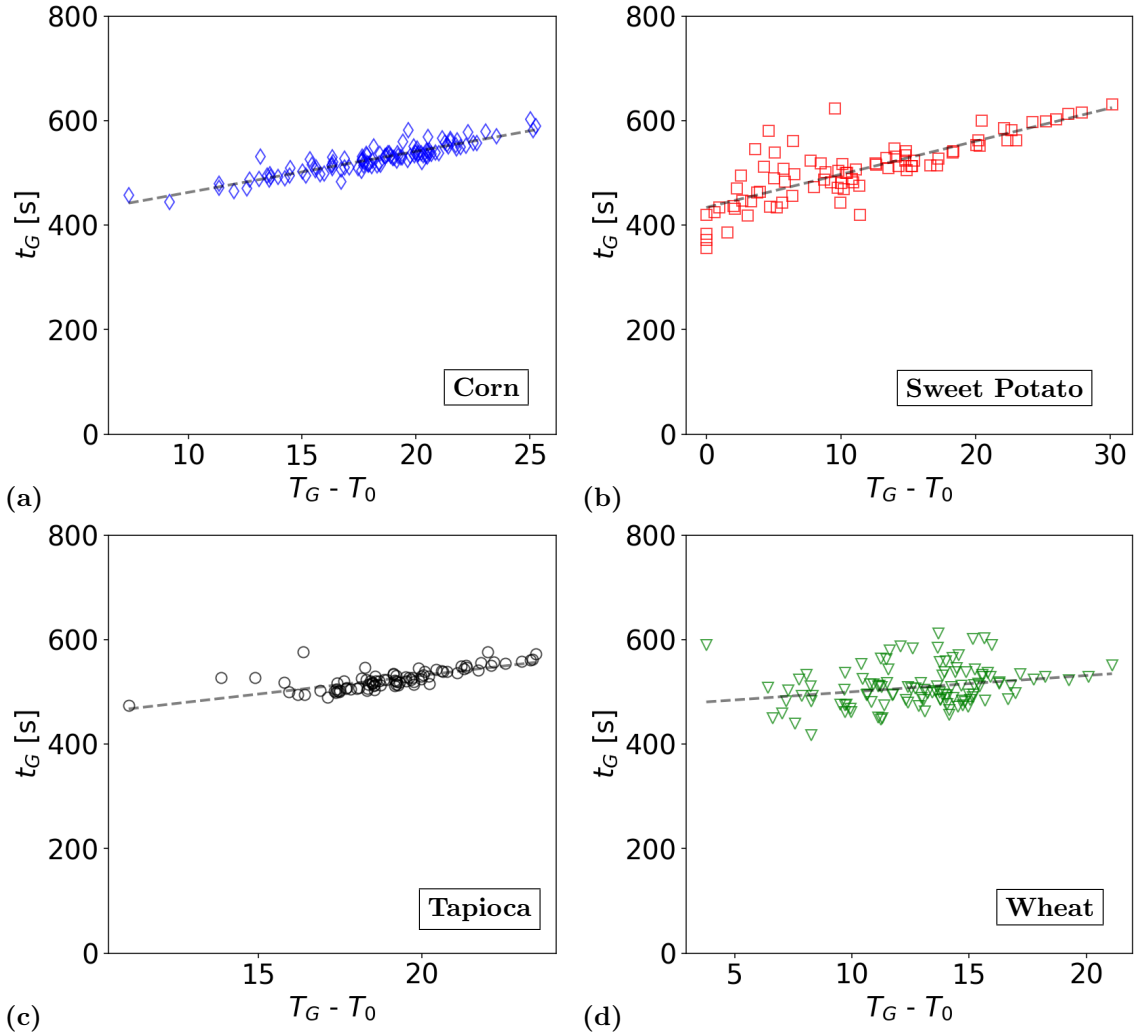

Figure 14: Swelling time t_G vs. gelatinization temperature difference, T_G-T_0, for (a) corn, (b) sweet potato, (c) tapioca, and (d) wheat gelatinized in water.

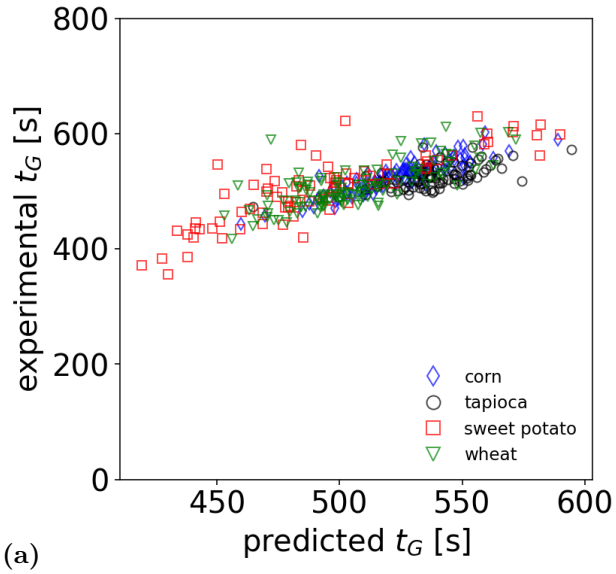

Figure 15: Comparison of t_G acquired experimentally, vs predicted t_G from Equation 6.

Table 3: Optimized constants from fitting Equation 6 for each starch type gelatinized in water, and for all of the starches considered together.

Test	k_1[s]	k_2	$k_3[\frac{s}{K}]$	r
Simulation [31]	15.8	0.732	2.14	-
Corn	617.95	0.091	7.70	0.923
Sweet Potato	575.21	0.269	7.31	0.849
Tapioca	633.40	0.063	6.98	0.770
Wheat	649.46	0.215	3.73	0.790
All Starches in Water	639.12	0.172	5.53	0.785

Finally, using Equation 6, we plotted the predicted t_G values calculated from the starch granule properties to the experimental t_G values we extracted from the Gompertz function in Figure 15. To optimize the line of best fit for each starch type and for all granules together, we adjusted the constants k_1, k_2, and k_3 from the original simulation values. These values and their corresponding correlation coefficients are summarized in Table 3.

In comparison to the optimized equation from the simulation (Equation 6), a disagreement is observed in the three values of fitted constants across the different starch types. We found that k_1 is more than an order of magnitude larger, k_2 is nearly an order of magnitude smaller, while k_3 is about three times larger than the simulation-derived values. We find that the differences in k_1 and k_2 are consistent with the swelling time being insensitive to the swelling ratio as seen in Figure 13. We suggest that this means that the swelling time is primarily determined by swelling temperature.

To discuss the differences in k_3, we first note that a linear ramp was used in this present study, while in the simulation, a parabolic function was used to heat the starches, where both of the functions increased the chamber temperature from 50 to 90°C within the same time period (Equation 1). This means that in the simulations there was a steeper initial heating rate, which might account for the smaller value of k_3. However, this difference between the heating profiles is likely not enough to account for the increase by about a factor of three in k_3 that we observe here. Nonetheless it is important to note the role of the heating profile on the measured swelling curve shape and its properties. We conclude that the correlation equation proposed by Li et al. does not match the experimental data and should not be used for predictions.

4. Conclusion

In this study, a ParCS apparatus was used to track and quantify the gelatinization properties of corn, sweet potato, tapioca, and type-A wheat starches in water and solutions of glucose and sucrose. We were able to partially accept our first hypothesis that the swelling curves of these starches can be collapsed onto a master curve by nondimensionalizing and shifting the data, based on only four parameters. However, we were surprised to find that the precise shape of the master curve was dependent on the starch type and *not* on the solution type. This caused us to reject the hypothesis that the swelling curve would be fundamentally altered by the presence of solutes.

After comparing the measured swelling time as a function of swelling ratio and gelatinization temperature, with the relationship predicted by Li et al. we had to reject our second hypothesis that the model was valid. Specifically, we did not observe a dependence of the swelling time on the swelling ratio as predicted by the model. We did observe a linear relationship between the swelling time and the gelatinization temperature, as predicted, but the slope was not the same.

In addition to testing our two hypotheses, we also achieved three things for the first time. First, we provided quantitative measurements showing that the intra-sample variability in the swelling ratio can be reduced by higher concentrations of glucose and sucrose. Second, we showed that even though solutes can alter the swelling temperature, they have only a minimal impact on the swelling rate. Third, we made the first measurements of an effective, diffusion coefficient of water in individual, intact starch granules. These measured diffusion coefficients were three orders of magnitude lower than that of pure water, and two orders lower than sugar in water. When comparing this work to predictions from theory, there is support for the hypothesis of swelling rate dependence on starch diffusivity, and likely the structuring and properties of the internal polymer network.

Altogether, this work demonstrates the effectiveness of the ParCS method in characterizing starch gelatinization across a wide range of starch types and processing conditions. By exploring both the intrinsic and extrinsic properties that influence starch swelling, these results contribute to gaining detailed fundamental understanding of the gelatinization process and the mechanisms involved. These insights are critical for further refinements and validation of first-principles models of gelatinization. In turn, this insight and subsequent models will support advances in a vast range of food and other industrial applications involving starch.

Declaration of competing interests

The authors declare no conflict of interest.

CRediT authorship contribution statement

Lily M.A. Santos O'Keefe: Conceptualization, Methodology, Formal analysis, Investigation, Writing – original draft, Writing – review and editing. **Yash Mali**: Software. **John M. Frostad**: Conceptualization, Methodology, Funding acquisition, Project administration, Supervision, Writing – original draft, Writing – review and editing.

Acknowledgements

The authors are grateful for support through funding from the Canada Foundation for Innovation John R. Evans Leaders Fund, the British Columbia Knowledge Development Fund, the Discovery Grant Program of the Natural Sciences and Engineering Research Council of Canada (NSERC) (Grant No. RGPIN-2024-04397), an NSERC Alliance Grant in collaboration with Ingredion Canada (ALLRP-566958-21), and an NSERC Undergraduate Student Research Award.

References

[1] D. French, Organization of starch granules, in: Starch: Chemistry and Technology, Elsevier, 1984, pp. 183–247. doi:10.1016/B978-0-12-746270-7.50013-6.

[2] T. A. Waigh, M. J. Gidley, B. U. Komanshek, A. M. Donald, The phase transformations in starch during gelatinisation: a liquid crystalline approach, Carbohydrate Research 328 (2) (2000) 165–176. doi:10.1016/S0008-6215(00)00098-7.

[3] A. Romano, A. Mackie, F. Farina, M. Aponte, F. Sarghini, P. Masi, Characterisation, in vitro digestibility and expected glycemic index of commercial starches as uncooked ingredients, Journal of Food Science and Technology 53 (12) (2016) 4126–4134. doi:10.1007/s13197-016-2375-9.

[4] S. Singh, N. Singh, N. Isono, T. Noda, Relationship of granule size distribution and amylopectin structure with pasting, thermal, and retrogradation properties in wheat starch, Journal of Agricultural and Food Chemistry 58 (2) (2010) 1180–1188. doi:10.1021/jf902753f.

[5] A. A. Wani, P. Singh, M. A. Shah, U. Schweiggert-Weisz, K. Gul, I. A. Wani, Rice starch diversity: Effects on structural, morphological, thermal, and physicochemical properties—A review, Comprehensive Reviews in Food Science and Food Safety 11 (5) (2012) 417–436. doi:10.1111/j.1541-4337.2012.00193.x.

[6] K. Zhang, D. Zhao, X. Zhang, L. Qu, Y. Zhang, Q. Huang, Effects of the removal of lipids and surface proteins on the physicochemical and structural properties of green wheat starches, Starch - Stärke 73 (1-2) (2021) 2000046. doi:10.1002/star.202000046.

[7] Z. Xu, X. Liu, M. Ma, J. He, Z. Sui, H. Corke, Reduction of starch granule surface lipids alters the physicochemical properties of crosslinked maize starch, International Journal of Biological Macromolecules 259 (2024) 129139. doi:10.1016/j.ijbiomac.2023.129139.

[8] M. Ma, Y. Wen, C. Zhang, Z. Xu, H. Li, Z. Sui, H. Corke, Extraction and characterization of starch granule-associated surface and channel lipids from small-granule starches that affect physicochemical properties, Food Hydrocolloids 126 (2022) 107370. doi:10.1016/j.foodhyd.2021.107370.

[9] X. Kong, J. Bao, H. Corke, Physical properties of amaranthus starch, Food Chemistry 113 (2) (2009) 371–376. doi:10.1016/j.foodchem.2008.06.028.

[10] W. Li, S. Sun, Z. Gu, L. Cheng, Z. Li, C. Li, Y. Hong, Effect of protein on the gelatinization behavior and digestibility of corn flour with different amylose contents, International Journal of Biological Macromolecules 249 (2023) 125971. doi:10.1016/j.ijbiomac.2023.125971.

[11] J. Man, L. Lin, Z. Wang, Y. Wang, Q. Liu, C. Wei, Different structures of heterogeneous starch granules from high-amylose rice, Journal of Agricultural and Food Chemistry 62 (46) (2014) 11254–11263. doi:10.1021/jf503999r.

[12] S. Helle, F. Bray, J.-L. Putaux, J. Verbeke, S. Flament, C. Rolando, C. D'Hulst, N. Szydlowski, Intra-sample heterogeneity of potato starch reveals fluctuation of starch-binding proteins according to granule morphology, Plants 8 (9) (2019) 324. doi:10.3390/plants8090324.

[13] S. Dhital, K. J. Shelat, A. K. Shrestha, M. J. Gidley, Heterogeneity in maize starch granule internal architecture deduced from diffusion of fluorescent dextran probes, Carbohydrate Polymers 93 (2) (2013) 365–373. doi:10.1016/j.carbpol.2012.12.017.

[14] M. C. Allan, B. Rajwa, L. J. Mauer, Effects of sugars and sugar alcohols on the gelatinization temperature of wheat starch, Food Hydrocolloids 84 (2018) 593–607. doi:10.1016/j.foodhyd.2018.06.035.

[15] C. Chen, G. Li, H. Corke, F. Zhu, Physicochemical properties of starch in sodium chloride solutions and sucrose solutions: Importance of starch structure, Food Chemistry 421 (2023) 136141. doi:10.1016/j.foodchem.2023.136141.

[16] T. J. Woodbury, S. L. Pitts, A. M. Pilch, P. Smith, L. J. Mauer, Mechanisms of the different effects of sucrose, glucose, fructose, and a glucose–fructose mixture on wheat starch gelatinization, pasting, and retrogradation, Journal of Food Science 88 (1) (2023) 293–314. doi:10.1111/1750-3841.16414.

[17] P. Perry, A. Donald, The effect of sugars on the gelatinisation of starch, Carbohydrate Polymers 49 (2) (2002) 155–165. doi:10.1016/S0144-8617(01)00324-1.

[18] I. D. Evans, D. R. Haisman, The effect of solutes on the gelatinization temperature pange of potato starch, Starch - Stärke 34 (7) (1982) 224–231. doi:10.1002/star.19820340704.

[19] S. Li, Z. Wang, D. Feng, Y. Pan, E. Li, J. Wang, C. Li, The important role of starch fine molecular structures in starch gelatinization property with addition of sugars/sugar alcohols, Carbohydrate Polymers 330 (2024) 121785. doi:10.1016/j.carbpol.2024.121785.

[20] S. Renzetti, I. A. Van Den Hoek, R. G. Van Der Sman, Mechanisms controlling wheat starch gelatinization and pasting behaviour in presence of sugars and sugar replacers: Role of hydrogen bonding and plasticizer molar volume, Food Hydrocolloids 119 (2021) 106880. doi:10.1016/j.foodhyd.2021.106880.

[21] G. P. Desam, O. G. Jones, G. Narsimhan, Prediction of the effect of sucrose on equilibrium swelling of starch suspensions, Journal of Food Engineering 294 (2021) 110397. doi:10.1016/j.jfoodeng.2020.110397.

[22] R. Bertrand, W. Holmes, C. Orgeron, C. McIntyre, R. Hernandez, E. D. Revellame, Rapid estimation of parameters for gelatinization of waxy corn starch, Foods 8 (11) (2019) 556. doi:10.3390/foods8110556.

[23] S. Watanabe, Y. Nishitsuji, K. Hayakawa, Y.-C. Shi, Pasting properties of A- and B-type wheat starch granules and annealed starches in relation to swelling and solubility, International Journal of Biological Macromolecules 261 (2024) 129738. doi:10.1016/j.ijbiomac.2024.129738.

[24] Y. Niu, Y. Zheng, X. Fu, D. Zeng, H. Liu, A novel characterization of starch gelatinization using microscopy observation with deep learning methodology, Journal of Food Engineering 327 (2022) 111057. doi:10.1016/j.jfoodeng.2022.111057.

[25] B. Pan, J. Tao, X. Bao, J. Xiao, H. Liu, X. Zhao, D. Zeng, Quantitative study of starch swelling capacity during

gelatinization with an efficient automatic segmentation methodology, Carbohydrate Polymers 255 (2021) 117372. doi:10.1016/j.carbpol.2020.117372.
[26] G. Zhong, Y. Liu, S. Zhang, J. Lia, Y. Wang, D. Zeng, H. Liu, Efficient and rapid assessment of starch gelatinization through intelligent methodologies, International Journal of Biological Macromolecules (2025) 142954doi:10.1016/j.ijbiomac.2025.142954.
[27] F. Deslandes, A. Plana-Fattori, G. Almeida, G. Moulin, C. Doursat, D. Flick, Estimation of individual starch granule swelling under hydro-thermal treatment, Food Structure 22 (2019) 100125. doi:10.1016/j.foostr.2019.100125.
[28] A. Palanisamy, F. Deslandes, M. Ramaioli, P. Menut, A. Plana-Fattori, D. Flick, Kinetic modelling of individual starch granules swelling, Food Structure 26 (2020) 100150. doi:10.1016/j.foostr.2020.100150.
[29] L. Mo, J. Cheon, J. M. Frostad, Quantifying and modeling the gelatinization properties of individual pulse-starch granules by ParCS, Food Hydrocolloids 135 (2023) 107896. doi:10.1016/j.foodhyd.2022.107896.
[30] D. T. Do, J. Singh, I. Oey, H. Singh, R. Y. Yada, J. M. Frostad, A novel apparatus for time-lapse optical microscopy of gelatinisation and digestion of starch inside plant cells, Food Hydrocolloids 104 (2020) 105551. doi:10.1016/j.foodhyd.2019.105551.
[31] B. Li, L. Mo, V. Narsimhan, G. Narsimhan, J. M. Frostad, A refined mechanistic model for swelling kinetics of starch granules, Soft Matter 21 (22) (2025) 4351–4367. doi:10.1039/D4SM00980K.
[32] K. S. Sandhu, N. Singh, N. S. Malhi, Physicochemical and thermal properties of starches separated from corn produced from crosses of two germ pools, Food Chemistry 89 (4) (2005) 541–548. doi:10.1016/j.foodchem.2004.03.007.
[33] O. K. Abegunde, T.-H. Mu, J.-W. Chen, F.-M. Deng, Physicochemical characterization of sweet potato starches popularly used in Chinese starch industry, Food Hydrocolloids 33 (2) (2013) 169–177. doi:10.1016/j.foodhyd.2013.03.005.
[34] E. Bromley, I. Hopkinson, Confocal microscopy of a dense particle system, Journal of Colloid and Interface Science 245 (1) (2002) 75–80. doi:10.1006/jcis.2001.8005.
[35] V. Ziegler, N. D. S. Timm, C. D. Ferreira, J. T. Goebel, R. S. Pohndorf, M. D. Oliveira, Effects of drying temperature of red popcorn grains on the morphology, technological, and digestibility properties of starch, International Journal of Biological Macromolecules 145 (2020) 568–574. doi:10.1016/j.ijbiomac.2019.12.198.
[36] D. Park, K. G. Allen, F. R. Stermitz, J. A. Maga, Chemical composition and physical characteristics of unpopped popcorn hybrids, Journal of Food Composition and Analysis 13 (6) (2000) 921–934. doi:10.1006/jfca.2000.0943.
[37] Y. Li, L. Zhao, L. Shi, L. Lin, Q. Cao, C. Wei, Sizes, components, crystalline structure, and thermal properties of starches from sweet potato varieties originating from different countries, Molecules 27 (6) (2022) 1905. doi:10.3390/molecules27061905.
[38] A. Rolland-Sabaté, T. Sánchez, A. Buléon, P. Colonna, B. Jaillais, H. Ceballos, D. Dufour, Structural characterization of novel cassava starches with low and high-amylose contents in comparison with other commercial sources, Food Hydrocolloids 27 (1) (2012) 161–174. doi:10.1016/j.foodhyd.2011.07.008.
[39] L. Ding, W. Liang, J. Qu, S. Persson, X. Liu, K. Herburger, J. J. K. Kirkensgaard, B. Khakimov, K. Enemark-Rasmussen, A. Blennow, Y. Zhong, Effects of natural starch-phosphate monoester content on the multi-scale structures of potato starches, Carbohydrate Polymers 310 (2023) 120740. doi:10.1016/j.carbpol.2023.120740.
[40] J. Y. Chung, A. J. Nolte, C. M. Stafford, Diffusion-controlled, self-organized growth of symmetric wrinkling patterns, Advanced Materials 21 (13) (2009) 1358–1362. doi:10.1002/adma.200803209.
[41] N. Liu, Q. Sun, Z. Yang, L. Shan, Z. Wang, H. Li, Wrinkled interfaces: Taking advantage of anisotropic wrinkling to periodically pattern polymer surfaces, Advanced Science 10 (12) (2023) 2207210. doi:10.1002/advs.202207210.
[42] A. Kirillov, E. Mintun, N. Ravi, H. Mao, C. Rolland, L. Gustafson, T. Xiao, S. Whitehead, A. C. Berg, W.-Y. Lo, P. Dollár, R. Girshick, Segment Anything (2023). doi:10.48550/ARXIV.2304.02643.
[43] X. Zhao, W. Ding, Y. An, Y. Du, T. Yu, M. Li, M. Tang, J. Wang, Fast Segment Anything (2023). doi:10.48550/ARXIV.2306.12156.
[44] Y. Zhang, P. Sun, Y. Jiang, D. Yu, F. Weng, Z. Yuan, P. Luo, W. Liu, X. Wang, ByteTrack: Multi-object tracking by associating every detection box, in: S. Avidan, G. Brostow, M. Cissé, G. M. Farinella, T. Hassner (Eds.), Computer Vision – ECCV 2022, Vol. 13682, Springer Nature Switzerland, Cham, 2022, pp. 1–21. doi:10.1007/978-3-031-20047-2_1.
[45] S. Suzuki, K. Be, Topological structural analysis of digitized binary images by border following, Computer Vision, Graphics, and Image Processing 30 (1) (1985) 32–46. doi:10.1016/0734-189X(85)90016-7.
[46] D. H. Douglas, T. K. Peucker, Algorithms for the reduction of the number of points required to represent a digitized line or its caricature, Cartographica: The International Journal for Geographic Information and Geovisualization 10 (2) (1973) 112–122. doi:10.3138/FM57-6770-U75U-7727.
[47] R. F. Tester, W. R. Morrison, Swelling and gelatinization of cereal starches. I. Effects of amylopectin, amylose, and lipids., Cereal Chemistry 67 (6) (1990) 551–557.
[48] P. Bowler, M. R. Williams, R. E. Angold, A hypothesis for the morphological changes which occur on heating lenticular wheat starch in water, Starch - Stärke 32 (6) (1980) 186–189. doi:10.1002/star.19800320603.
[49] P. Malumba, N. Jacquet, G. Delimme, F. Lefebvre, F. Béra, The swelling behaviour of wheat starch granules during isothermal and non-isothermal treatments, Journal of Food Engineering 114 (2) (2013) 199–206. doi:10.1016/j.jfoodeng.2012.08.010.
[50] M. M. Bean, W. T. Yamazaki, Wheat starch gelatinization in sugar solutions. I. Sucrose: Microscopy and viscosity effects., Cereal Chemistry 55 (6) (1978) 936–944.
[51] A. G. Teobaldi, G. N. Barrera, L. S. Sciarini, P. D. Ribotta, Pasting, gelatinization, and rheological properties of wheat starch in the presence of sucrose and gluten, European Food Research and Technology 247 (5) (2021) 1083–1093. doi:10.1007/s00217-021-03689-y.
[52] A. Gunaratne, S. Ranaweera, H. Corke, Thermal, pasting, and gelling properties of wheat and potato starches in the

presence of sucrose, glucose, glycerol, and hydroxypropyl β-cyclodextrin, Carbohydrate Polymers 70 (1) (2007) 112–122. doi:10.1016/j.carbpol.2007.03.011.

[53] E. Chiotelli, A. Rolée, M. Le Meste, Effect of sucrose on the thermomechanical behavior of concentrated wheat and waxy corn starch-water preparations, Journal of Agricultural and Food Chemistry 48 (4) (2000) 1327–1339. doi:10.1021/jf990817f.

[54] G. Richardson, M. Langton, A. Bark, A. Hermansson, Wheat starch gelatinization — the effects of sucrose, emulsifier and the physical state of the emulsifier, Starch - Stärke 55 (3-4) (2003) 150–161. doi:10.1002/star.200390029.

[55] T. J. Woodbury, E. Grush, M. C. Allan, L. J. Mauer, The effects of sugars and sugar alcohols on the pasting and granular swelling of wheat starch, Food Hydrocolloids 126 (2022) 107433. doi:10.1016/j.foodhyd.2021.107433.

[56] T. Zhang, M. Wu, W. Wei, T. He, X. Zhang, H. Xu, D. Sun, Multiscale insights into the role of water content in the extrusion-crosslinked starch, International Journal of Biological Macromolecules 307 (2025) 142118. doi:10.1016/j.ijbiomac.2025.142118.
URL https://linkinghub.elsevier.com/retrieve/pii/S0141813025026704

[57] M. C. Allan, M. Chamberlain, L. J. Mauer, Effects of sugars and sugar alcohols on the gelatinization temperatures of wheat, potato, and corn starches, Foods 9 (6) (2020) 757. doi:10.3390/foods9060757.

[58] X. Zhang, Q. Tong, W. Zhu, F. Ren, Pasting, rheological properties and gelatinization kinetics of tapioca starch with sucrose or glucose, Journal of Food Engineering 114 (2) (2013) 255–261. doi:10.1016/j.jfoodeng.2012.08.002.

[59] D.-N. Zhou, B. Zhang, B. Chen, H.-Q. Chen, Effects of oligosaccharides on pasting, thermal and rheological properties of sweet potato starch, Food Chemistry 230 (2017) 516–523. doi:10.1016/j.foodchem.2017.03.088.

[60] T. J. Woodbury, L. J. Mauer, Oligosaccharide, sucrose, and allulose effects on the pasting and retrogradation behaviors of wheat starch, Food Research International 171 (2023) 113002. doi:10.1016/j.foodres.2023.113002.

[61] V. Singh, S. Ali, R. Somashekar, P. Mukherjee, Nature of crystallinity in native and acid modified starches, International Journal of Food Properties 9 (4) (2006) 845–854. doi:10.1080/10942910600698922.

[62] J. W. Donovan, K. Lorenz, K. Kulp, Differential scanning calorimetry of heat-moisture treated wheat and potato starches, Cereal Chemistry 60 (5) (1983) 381–387.

[63] W. S. Ratnayake, C. Otani, D. S. Jackson, DSC enthalpic transitions during starch gelatinisation in excess water, dilute sodium chloride and dilute sucrose solutions, Journal of the Science of Food and Agriculture 89 (12) (2009) 2156–2164. doi:10.1002/jsfa.3709.

[64] T.-T. Huang, D.-N. Zhou, Z.-Y. Jin, X.-M. Xu, H.-Q. Chen, Effect of debranching and heat-moisture treatments on structural characteristics and digestibility of sweet potato starch, Food Chemistry 187 (2015) 218–224. doi:10.1016/j.foodchem.2015.04.050.

[65] L. Shi, K. Guo, X. Xu, L. Lin, X. Bian, C. Wei, Physicochemical properties of starches from sweet potato root tubers grown in natural high and low temperature soils, Food Chemistry: X 22 (2024) 101346. doi:10.1016/j.fochx.2024.101346.

[66] M. Kaur, D. P. S. Oberoi, D. S. Sogi, B. S. Gill, Physicochemical, morphological and pasting properties of acid treated starches from different botanical sources, Journal of Food Science and Technology 48 (4) (2011) 460–465. doi:10.1007/s13197-010-0126-x.

[67] W. F. Breuninger, K. Piyachomkwan, K. Sriroth, Chapter 12 - Tapioca/cassava starch: Production and use, in: J. BeMiller, R. Whistler (Eds.), Starch (Third Edition), third edition Edition, Food Science and Technology, Academic Press, San Diego, 2009, pp. 541–568. doi:https://doi.org/10.1016/B978-0-12-746275-2.00012-4.

[68] V. Vamadevan, E. Bertoft, Observations on the impact of amylopectin and amylose structure on the swelling of starch granules, Food Hydrocolloids 103 (2020) 105663. doi:10.1016/j.foodhyd.2020.105663.

[69] M. Holz, S. R. Heil, A. Sacco, Temperature-dependent self-diffusion coefficients of water and six selected molecular liquids for calibration in accurate 1H NMR PFG measurements, Physical Chemistry Chemical Physics 2 (20) (2000) 4740–4742. doi:10.1039/b005319h.

[70] M. Rampp, C. Buttersack, H.-D. Lüdemann, c,T-Dependence of the viscosity and the self-diffusion coefficients in some aqueous carbohydrate solutions, Carbohydrate Research 328 (4) (2000) 561–572. doi:10.1016/S0008-6215(00)00141-5.

[71] G. Saravacos, V. Karathanos, S. Marousis, Diffusion of water in starch materials, in: Developments in Food Science, Vol. 29, Elsevier, 1992, pp. 329–340. doi:10.1016/B978-0-444-88834-1.50032-6.

[72] R. B. Leslie, P. J. Carillo, T. Y. Chung, S. G. Gilbert, K. Hayakawa, S. Marousis, G. D. Saravacos, M. Solberg, Water diffusivity in starch-based systems, in: H. Levine, L. Slade (Eds.), Water Relationships in Foods, Vol. 302, Springer US, Boston, MA, 1991, pp. 365–390, series Title: Advances in Experimental Medicine and Biology. doi:10.1007/978-1-4899-0664-9_21.

[73] V. T. Karathanos, G. K. Vagenas, G. D. Saravacos, Water diffusivity in starches at high temperatures and pressures, Biotechnology Progress 7 (2) (1991) 178–184. doi:10.1021/bp00008a013.